INVESTIGATION INTO DIFFERENT CORE CONFIGURATIONS OF THE SAFARI-1 RESEARCH REACTOR

C. ORION PHILLIPS

Dissertation submitted in partial fulfilment of the requirements for the degree Magister Scientiae in Reactor Science at North-West University, Potchefstroom campus.

Supervisor: Prof. H. Moraal
Co-supervisor: Dr. A. L. Graham

November 2007

ACKNOWLEDGEMENTS

In keeping with my faith and acknowledgement of the author of knowledge, God Almighty, I express my gratitude for the strength to complete this work. My sentiments can be expressed as follows:

"Science opens new wonders to our view; she soars high, and explores new depths; but she brings nothing from her research that conflicts with divine revelation. Ignorance may seek to support false views of God by appeals to science, but the book of nature and the written word shed light upon each other. We are thus led to adore the Creator and to have an intelligent trust in His word." – Ellen G. White.

I wish to express my gratitude to my colleagues at Necsa, R. H. Prinsloo and Dr. A. L. Graham who demonstrated dedication in assisting an older student, also to Dr. D. I. Tomašević who provided a high standard and guidance in the field of reactor science.

For the support of my family, I am truly thankful, especially to my wife Ursula who had to forego many hours without me while I worked on this dissertation. I also thank my two sons, David and Chase, who experienced an "absent father"; however, the family will also benefit now that I have reached this milestone. Finally, my Dad, who came to my assistance during times of crisis and whose health is failing now, provided the platform for me.

ABSTRACT

In-core fuel management consists of the placement of fuel in a suitable mass distribution that ensures that core performance is optimised, while technical and safety constraints are also satisfied. In addition, from an operational point of view, the selected mass distribution should result in efficient use of the fuel and tend to bring about uniformity in the neutron flux distribution. As reactor cores are designed in terms of discrete, reloadable fuel assemblies, the problem becomes one of determining the optimal locations of fuel assemblies of different burn-ups, thereby defining a core-loading pattern. In this dissertation, two core configurations are investigated in order to find the best arrangement of assemblies in the core subject to particular operational constraints. In either case, considerations regarding specific reloads include the following: the number of fresh fuel assembles to be used; whether to load fresh control rod assemblies; the remaining ^{235}U content of the nearly depleted fuel assemblies to be reinserted; and the distribution of ^{235}U content amongst the assemblies making up the core. Because of the current reload strategy at the SAFARI-1 research reactor, a surplus of spent fuel assemblies with between 120 g and 140 g ^{235}U has accumulated. In view of the high premium placed on highly enriched uranium fuel utilization and the high value of fissile material it has become imperative to investigate whether these assemblies can be burned as part of normal operations in the reactor core. However, it is important to investigate the feasibility of such a fuel management proposition before implementing it. The question therefore arises as to the most suitable location in the core to place assemblies within the given ^{235}U mass range. This objective should be achieved while maintaining the thermal neutron flux levels in the SAFARI-1 irradiation positions and without compromising fuel economy. OSCAR-3 is a 3-D neutronic computational tool that is used in this investigation to simulate the core configurations. The dissertation describes the design parameters and operational limits and conditions of the research reactor, before developing the theoretical concepts that will be used as a basis for the neutronic parameters that are generated by the code. The features of the 3-D OSCAR-3 code are described in order to establish its suitability to solve the problem that is being investigated. Finally, the results obtained from the code calculations are used to recommend an appropriate plan of action for the utilization of nearly spent fuel that has accumulated over time with the operation of SAFARI-1.

SAMEVATTING

Die effektiewe binne-kern bestuur van kernreaktorbrandstof vereis 'n strategie wat tergelykertyd reaktorveiligheid en neutronbruikbaarheid verseker.

Aangesien die brandstof (hoofsaaklik ^{235}U as splytingsmateriaal) in elemente versamel word, kan ons hierdie probleem herformuleer as die soeke na 'n brandstofelement-herladingspatroon wat met reëlmaat vir reaktorsiklusherlading gebruik kan word.

In hierdie verhandeling word twee onafhanklike reaktorkernherladingsskemas ondersoek en vergelyk na gelang van operasionele beperkings.

Tipiese keuses wat aan die begin van 'n reaktorsiklus gemaak moet word, sluit aspekte in soos die hoeveelheid vars brandstof- en beheerstaaf elemente (300 g ^{235}U en 200 g ^{235}U onderskeidelik) wat tydens herlading gebruik moet word, die spesifieke elemente wat verwyder moet word, en die plasing van die finale stel elemente in die kern.

In hierdie verhandeling word bostaande probleem spesifiek vir die Suid-Afrikaanse SAFARI-1 reaktor bespreek. 'n Verdere interessante vereiste handel oor 'n baie praktiese situasie aangaande die gebruik van 'n groot aantal ouer brandstof-elemente (met ^{235}U massas tussen 120 g en 140 g) in toekomstige siklusse. Hierdie elemente is tipies naby aan hulle verbrandingsperk, maar kan moontlik nog in spesifieke gevalle gebruik word. Uit die kosteperspektief van hoogverrykte uraan sal herladingsstrategieë wat die verdere gebruik van ou elemente insluit, baie waardevol wees.

In teenstelling met hierdie voordeel, kan die gebruik van ouer elemente die neutron-vloedvlakke in bestralingsposisies negatief beïnvloed. Aangesien een van die hooftoepassings van SAFARI-1 die verkoop van verskeie bestralingsprodukte insluit, sal die die voor- en nadele van die bogenoemde strategie versigtig oorweeg moet word.

Die primêre program waarmee die nodige studies uitgevoer word, is die neutroniese simulasiesagtewarepakket, OSCAR-3, wat as 'n reël vir die SAFARI-1 berekenings-ondersteuning gebruik word.

Die verhandeling se verloop is soos volg: Die SAFARI-1 kernreaktor, met operasionele limiete en bedryfsaspekte, word aanvanklik bespreek. Dit word gevolg deur 'n beskrywing van die nodige teoretiese agtergrond vir hierdie werk, met spesifieke verwysings na die metodes wat in die OSCAR-3 sisteem toegepas word. Die fokus van die verhandeling word hierna d.m.v numeriese resultate en besprekings oor die toepaslikheid van die verskeie herladingsstrategieë gegee. Ter afsluiting word gefundeerde voorstelle en aanbevelings aangaande 'n moontlike verbeterde herladingsstrategie gemaak.

TABLE OF CONTENTS

ACKNOWLEDGEMENTS ii

ABSTRACT iii

SAMEVATTING iv

TABLE OF CONTENTS vi

LIST OF FIGURES viii

LIST OF TABLES ix

CHAPTER 1 INTRODUCTION 10

1.1 Overview 10
1.2 Problem statement 10
1.3 Literature review 11
1.4 Previous research conducted 12
1.5 Field of study 12
1.6 Methods and procedures used in this investigation 12
1.7 Definitions of terms 15
1.8 Approach adopted 17
1.9 Structure of the dissertation 17

CHAPTER 2 THE SAFARI-1 RESEARCH REACTOR 19

2.1 Introduction 19
2.2 Design parameters of the reactor core 19
2.3 Operational limits and conditions 20
2.4 An in-core fuel management plan 23
2.5 Fuel specification 26
2.6 Core configuration under investigation 27

CHAPTER 3 THEORETICAL BACKGROUND 30

3.1 Equation for describing the neutron distribution in the core 30
3.2 Power distribution 29
3.3 Fuel temperature limit 34
3.4 Depletion analysis 36
3.5 The equilibrium cycle 41
3.6 Power-peaking effects 41
3.7 Neutron leakage 42
3.8 The multiplication factor 42
3.9 Reactivity control 43
3.10 Fuel loading variables and constraints 44
3.11 The fuel arrangement 45
3.12 Effect of neutron fluence 46
3.13 Conclusion 47

CHAPTER 4 THE CORE FOLLOW CALCULATIONAL SYSTEM 49

4.1 Introduction 49
4.2 MGRAC 50
4.3 SHUFFLE 52
4.4 Application of OSCAR-3 53

CHAPTER 5 AN EQUILIBRIUM CORE STUDY **54**
5.1 Foreword to study 54
5.2 Fuel loading strategy 55
5.3 The most likely high-mass fuel assembly locations 55
5.3 The change in beginning-of-cycle mass 57
5.4 The change in the relative assembly power density 58
5.5 The change in the mass discharged from the core 61
5.6 The change in the thermal flux at irradiation position G3 62
5.7 Conditions of an equilibrium core 63
5.8 Change in control rod positions 63
5.9 Conclusion 66

CHAPTER 6 RESULTS AND DISCUSSIONS **67**
6.1 Introduction 67
6.2 Fissile mass distribution 67
6.3 Thermal fluxes 72
6.4 Fast fluxes 77
6.5 Depletion in cores 79
6.6 Reactivity control parameters 80
6.7 Fuel economy 80
6.8 Summary

CHAPTER 7 CONCLUSION AND RECOMMENDATIONS **80**
7.1 Introduction 80
7.2 Comparison between the two core configurations 80
7.3 Recommended core configuration 86
7.4 Future research 87
7.5 Conclusion 88

APPENDIX A **80**
APPENDIX B **87**

REFERENCES **100**

LIST OF FIGURES

Figure 1.1 Procedure for evaluating a core configuration

Figure 2.1 The SAFARI-1 reference core configuration

Figure 2.2 The SAFARI-1 core configuration 4

Figure 4.1 The OSCAR-3 design consisting of four sub-systems

Figure 5.1 The graph of the relative assembly power density at location E4

Figure 5.2 The graph of the change in beginning-of-cycle mass for 30 cycle iterations

Figure 6.1 The fissile mass distribution of the reference core

Figure 6.2 The fissile mass distribution of the core with the depleted masses in the central region of the core

Figure 6.3 The fissile mass distribution of the core with nearly depleted fuel assemblies on the western side of the core

LIST OF TABLES

Table 2.1 Operating information of the SAFARI-1 research reactor

Table 2.2 Design parameters of the SAFARI-1 20 MW research reactor

Table 2.3 Loading sequence for the core in Figure 2.1

Table 2.4 Highly enriched fuel specification

Table 3.1 Burnup steps for a 30-day operating cycle

Table 3.2 Constraints for the core configurations

Table 4.1 Levels for six energy groups

Table 5.1 Core operating parameters

Table 5.2 Analysis of the loading locations using the strat mode of OSCAR-3

Table 5.3 Mass discharged for cycle 16 to 25

Table 5.4 Thermal flux from cycle 16 to 25

Table 5.5 Control rod positions per burnup step for cycle 20 to 25

Table 5.6 BOC mass of the reactor core

Table 6.1 The mass distribution of Core A for the lowest mass to highest mass

Table 6.2 Thermal fluxes in the irradiation positions of the three different cores

Table 6.3 Comparison between thermal fluxes in reference core with Core A

Table 6.4 Comparison between thermal fluxes for the core box between the reference core and Core A

Table 6.5 Thermal fluxes in the hydraulic rabbit position for three cores

Table 6.6 Thermal flux on the poolside of the cores

Table 6.7 Thermal flux in the rig irradiation positions

Table 6.8 Thermal fluxes in irradiation positions, B8, D8, and F8 per layer for reference core

Table 6.9 Thermal fluxes in the irradiation positions, C3, E3, G3 per layer for reference core

Table 6.10 Thermal fluxes in irradiation positions, B8, D8, F8 per layer for recommended core

Table 6.11 Thermal fluxes in the irradiation positions, C3, E3, G3 per layer for recommended core

Table 6.12 Comparison between fast fluxes for core box between the reference core and Core A

Table 6.13 Comparison between fast fluxes for different cores

Table 6.14 Depletion in central region of core average for three cores

Table 6.15 Depletion at the periphery of the core for three cores

Table 6.16 Reactivity control parameters for the reference core and the recommended core

Table 6.17 Breakdown by mass over the depletion range for the reference core

Table 6.18 Breakdown by mass over the depletion range for the recommended core

CHAPTER 1 INTRODUCTION

1.1 Overview

In order to achieve optimum reactor core performance and minimise fuel costs, careful attention must be given to the management of the fuel in the reactor core. An essential element of this task lies in the need to determine the most favourable distribution of fuel in the initial and reload cores, which is in essence an extremely complex undertaking. This involves, inter alia, the core configuration and composition, reactivity control, the coupling between neutronics and thermal-hydraulics and operational requirements. The primary global variables under consideration for such a task are the cycle length of the core, the loading pattern selected, the power level of the core, and the fuel management strategy deployed to achieve optimum core performance.

The core management objectives of a given configuration are assessed by a detailed neutronic analysis. The resulting reactor physics variables play a pivotal role in the decision-making regarding the management of the core. This consideration will serve as a basis for determining the suitability of a core configuration in this dissertation.

1.2 Problem statement

The investigation into different core configurations for the SAFARI-1 research reactor is essential for effective core management as well as reactor core performance. The relevant parameters for each core configuration must be evaluated in order to arrive at operational cores that are consistent with the needs for efficient and effective operation. New core designs that exhibit stable characteristics form the basis for determining core performance in comparison to the past performance of the research reactor. In particular, a selected core configuration will be investigated in order to establish the preferred position for burning nearly depleted fuel assemblies. The fuel assemblies can be placed either in the central region of the core or on the periphery. It is then necessary to demonstrate that the selected core configurations meet the required criteria of core performance, safe operation, core uniformity, and lastly, but importantly, economical operation.

At the present time, there has been an accumulation of nearly spent fuel assemblies between 120 g to 140 g. These assemblies have accumulated due to the manner in which the fuel

assemblies in the core have been depleted over time. In terms of ensuring that valuable fuel material is optimally utilised it has at this time become important for the SAFARI-1 operation to ensure that these fuel assemblies are also used. This matter is specifically also attendant to the utilisation of highly enriched uranium (HEU) at the South African Nuclear Energy Corporation (Necsa). As part of a comprehensive project, involving the utilisation of HEU this investigation has become necessary for Necsa.

1.3 Literature review

This dissertation is primarily concerned with investigating suitable loading patterns for a selected operational need at SAFARI-1. As such, literature has been chosen that is appropriate to the topic under consideration. At first, it was essential to understand what physical parameters will be used to determine the appropriate loading pattern. After this had been established, it was necessary to link the reactor core variables to the appropriate scientific concepts that are dealt with in the literature. This is important so that the correct understanding could be developed around the problem under consideration. Sources were found that would therefore provide a basis for the topic being investigated.

The need to establish the use of the OSCAR-3 computational code for analysing problems associated with SAFARI-1 was also incorporated. The selected literature demonstrates the suitability of OSCAR-3 in solving problems of this nature. At the same time, these sources provide insight into the practical applications of the code. The literature also discusses the reactor physics parameters obtained with the code in light of the characterization of the reactor core performance. It shows which treatment is appropriate for neutronic analysis when considering the selection of a suitable loading arrangement.

It is important to provide sufficient theoretical background to the problem being investigated so that sound technical judgment can be applied. Using the theory as a basis, the reasoning that is then applied to the problem being investigated should be justified.

As will be seen in the text, the scope of this dissertation deals with considering particular loading patterns. This type of investigation involves calculating fuel cycle variables and evaluating these within the context of the feasibility of the arrangement. The literature chosen supports this purpose and has been carefully selected to provide the exact understanding to

do so. It therefore serves to ensure the appropriate technical integration as a whole to the topic under consideration.

1.4 Previous research conducted

Previous research undertaken does not directly address the problem under investigation. However, there was a need to reference research that had a bearing on the insights and outcomes that were required in this study. Scientific literature was therefore selected that would throw light on the problem, and these are listed in the bibliography. It was, however, essential to study research indicating how neutronic analysis may be used for decision making in regard to a core configuration. There was also a need to evaluate research that has been conducted in order to determine methods used in optimising nuclear fuel management. Insights were also gathered on the technical detail appropriate to bolstering arguments for core configurations and loading patterns that can be used by SAFARI-1.

1.5 Field of study

The fundamental scientific principles covered in this dissertation are based on concepts and tools derived from reactor physics theory. In this dissertation, the application of neutronic analysis of a reactor, in particular a research reactor is carried through to the level of establishing in-core fuel management plans adapted to the operational needs of the reactor. With respect to the operating requirements of the research reactor, an optimisation approach is required. Flowing from this is the need to integrate neutronic analysis with the economics of fuel cycle costs. The disciplines involved are essentially aimed at understanding the behaviour of neutrons in the reactor core using nuclear reactor theory while applying the constraints imposed by economics associated with fuel management during safe operation. In addition, the effect of depletion analysis is also applied in the determination of selecting appropriate locations for partially depleted fuel. Nuclear safety is an essential component of this analysis with the primary purpose of preventing fuel failure during operation.

1.6 Methods and procedures used in this investigation

The basis of the methods used in this dissertation is to start the investigation by evaluating available SAFARI-1 reactor core data. The reactor core data provides an indication of the mass distribution for cores that have been in operation. The fuel economy and performance

of these cores, including power distributions, are regarded as baseline indicators for comparison with new core designs.

When the proposed cores are loaded, similar mass distributions are adopted and the following factors are taken into consideration:

- The beginning-of-cycle ^{235}U mass.
- The requirement for the control rods to travel along a desired distance to end-of-cycle.
- The maximum power peaking factor allowable.

The above parameters are used as screening criteria before a more detailed analysis is conducted. Should these criteria be met and the calculated neutronic behaviour is acceptable, further calculations are done to characterise the core.

The detailed neutronic analysis, which is discussed in Chapter 6, is used to determine the suitability of the proposed core configuration, taking into account a number of factors, such as the in-core fuel management plan, the safety regime for operation, technical constraints that are present, and importantly, the neutronic behaviour of the core. The procedure adopted for evaluating a core configuration is found below in Figure 1.1.

Figure 1.1 Procedure for evaluating a core configuration

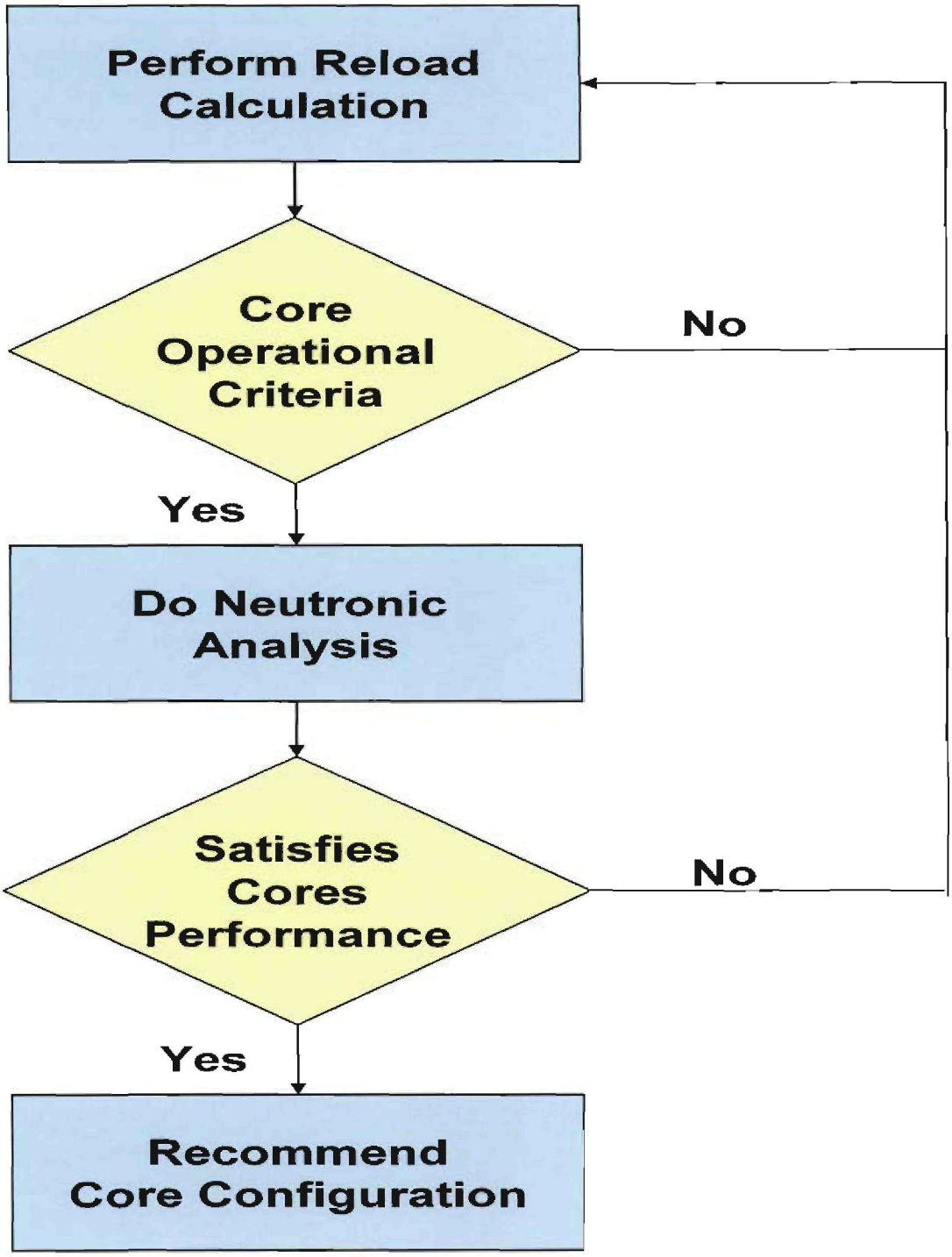

1.7 Definitions of terms

Excess reactivity:	The core reactivity present with all control elements withdrawn from the core.
Shutdown margin:	The negative reactivity of the core present when all control elements have been fully inserted to achieve minimum core multiplication.
Control element worth:	The reactivity worth of an individual control element induced in the core by full insertion of the element.
Multiplication factor:	The ratio of the number of neutrons in two successive fission neutron generations.
Effective multiplication: factor:	The multiplication factor characterising a finite system and denoted by k_{eff}.
Neutron leakage:	The neutrons that leak out of the reactor and are lost to the chain reaction.
Power peaking factor:	The ratio between the maximum power density and the average power density in the core.
Power distribution:	The spatial distribution of power in a given core configuration operating under steady-state conditions.
Power density:	The power generation per unit volume of the reactor core.
Cycle length:	The period of operation of a reactor with a given core loading.

Fluence:	A measure of time-integrated neutron flux.
Flux:	The amount of neutrons flowing across a square centimetre per unit time.

1.8 Approach adopted

The approach adopted is to investigate alternative core configurations for the SAFARI-1 reactor based on reactor physics principles. It is imperative to ensure that underlying assumptions about the reactor core are founded on appropriate neutronic analysis fundamentals, as are any changes that are proposed. Such changes must also comply with the operating philosophy that has been adopted for the reactor, based on the expertise developed over the years of operation. Since a lot is understood about the current operating regime of the reactor, it will be essential to integrate the changes proposed with the criteria that have been applied for efficient operation. The approach therefore relies on heuristic factors and those that involve scientific analysis.

The operational limits and conditions of the reactor provide a framework within which reactor core configurations can be evaluated. These limits and conditions are based on the Safety Analysis Report [13] and comply with the reactor design constraints.

1.9 Structure of the dissertation

Chapter 2: Chapter 2 of this dissertation presents a brief description of the SAFARI-1 research reactor. The design parameters are provided as an indication of the values that will govern the safe operation of the reactor. The characteristics of the reference core are also given since this information serves as basis for the cores that are evaluated in the remainder of the dissertation.

Chapter 3: Chapter 3 is primarily concerned with the theoretical basis of the problem being investigated. The treatment of advanced nodal diffusion theory is crucial for the understanding of the method of calculation used in performing the core analysis. Theoretical discussions are further pursued in respect of the parameters that will be evaluated later in the dissertation. The theory discussed together with the results obtained is the means of exercising sound technical judgement required to evaluate the various core configurations. The results obtained can also be explained in the context of the theory.

Chapter 4: Chapter 4 describes the features of OSCAR-3 used to characterise the neutron behaviour for the various core configurations that are investigated. The essential qualitative aspects of the computer codes are described so that the reader is able to understand its use.

Chapter 5: Chapter 5 deals with a process that was followed to reach an equilibrium core using the OSCAR-3 core analysis capability. Qualitative results are analysed in order to ascertain whether the core has reached equilibrium. This section can be published separately as a paper with some minor changes.

Chapter 6: Chapter 6 is central to this dissertation and is devoted to the results obtained from the neutronic analysis of the various configurations. The results and findings of the cores are discussed. The basis for the technical judgement of the cores is motivated in this part of the dissertation.

Chapter 7: Chapter 7 of this dissertation details the discussions, recommendations and conclusion of the investigation that has been undertaken. The adequacy of the recommended core configuration is discussed here. This chapter examines whether the research aims and objectives have been achieved. The specific objectives are reviewed as they provide an essential basis for the suitability of the core that is proposed.

CHAPTER 2 THE SAFARI-1 RESEARCH REACTOR

2.1 Introduction

The SAFARI-1 research reactor is a 20 MW tank-in-pool reactor owned and operated by the South African Nuclear Energy Corporation (Necsa) at its Pelindaba site near Pretoria, South Africa. The present core layout is an 8 x 9 grid housing 26 fuel elements, 5 control rods, and 1 regulating rod, in-core irradiation facilities and reflector elements. The core is fuelled with Material Test Reactor (MTR) type fuel elements comprising 19 flat plates each. The reactor vessel is cylindrical in shape except for one flattened side, which is also the wall of the rectangular core box adjacent to the poolside facility. This large ex-core poolside facility allows irradiations to be performed in relatively high neutron fluxes since it is directly adjacent to the fuel assembly region of the core. The reactor is also equipped with a number of neutron beam tubes that are used for neutron radiography, neutron scattering and prompt gamma neutron activation, while the hydraulic and pneumatic rabbit facilities make provision for the irradiation of various material samples [5].

The table below provides some important operating information of the SAFARI-1 research reactor.

Table 2.1: Operating Information of SAFARI-1 research reactor

Reactor type	Oak Ridge Reactor - Material Test Reactor
Initial criticality	March 1965
Operational status	Operating
Maximum thermal flux (n/cm^2/s)	2,5x10^{14} (neutron energies up to 0.625 eV)
Maximum fast flux (n/cm^2/s)	3,3x10^{14} (neutron energies above 0.625 eV)
Reactor power level	20 MW
Reactor vessel replacement	None

2.2 Design parameters of the reactor core

The table below provides an indication of important design parameters of the SAFARI-1 research reactor that will be used in the investigation in order to determine a suitable core configuration [13].

Table 2.2 20 MW Research Reactor-General description of design parameters

Fuel element	MTR-type element
Enrichment	87% - 93%
Number of fuel plates: Standard fuel element Control fuel element	 19 flat plates 15 flat plates
Plate dimensions	Standard MTR-plate
Fuel loading Standard fuel elements Control rod elements Regulating rod element	 300 g of ^{235}U 200 g of ^{235}U 200 g of ^{235}U
Core size	26 Fuel elements 5 Control rod elements 1 Regulating rod element
Core geometry: Position of irradiation channels	 C3 B6 B8 E3 D6 D8 G3 F6 F8
Grid plate	8 x 9
Desired average burn-up of ^{235}U, as restricted by the licence	Average burnup shall not exceed 80%. Normal burnup between 60% and 70% is expected.
Fuel shuffling	3 fresh fuel assemblies each reload
Control rod shuffling	1 fresh fuel assembly each reload
Reflector	2 Core sides reflected by Beryllium and water.
Thermal-Hydraulic data: Coolant flow rate Core inlet temperature	 2950 m^3/h 40° C

2.3 Operational limits and conditions

The following generic requirements pertaining to safe operation of the research reactor are provided [3]:

- A set of operational limits and conditions important to reactor safety, including safety limits, safety system settings, limiting conditions for safe operation and surveillance requirements acceptable to the regulatory body are established. The

operating staff shall ensure that the reactor is operated in accordance with the limits and conditions of the reactor throughout the life of the reactor.

- Core management is the strategy used to produce safe operational cores consistent with the needs of the operational requirements of the facility. It involves the determination by calculations often using validated methods and codes, of the location for fuel, reflectors, safety actuation devices, experimental devices and sometimes moderators in appropriate locations in the core.

- All core configurations shall be established in accordance with the design intent and assumptions as specified in the operational limits and conditions.

- Operational limits and conditions shall be established and procedures written for dealing with fuel element failures in order to minimize radioactive fission product releases from the fuel.

The actual relevant operational limits and conditions for the SAFARI-1 research reactors are as follows [13]:

Maximum and minimum number of fuel elements

- The reactor core shall not be made critical for normal operation if the core contains less than 26 fuel elements or more than 31 fuel elements. Fewer than 26 fuel elements leads to average power loadings outside the scope of the current safety analysis.

Number of control rods

- The reactor core shall contain 6 control rods, which shall be located in core positions C5, C7, E5, E7, G5, and G7, as illustrated in Figure 2.1. The control rod in position E5 shall be designated as the "regulating rod" and shall be coupled to the auto control system for automatic control of the reactor power.

Average and peak fuel element power

- The average fuel element power has been shown in the safety analysis to be compatible with the coolant flow rates. The neutronic power peaking factors for any given core loading shall be determined either experimentally or by calculation, and shall not cause the peak cladding temperature limit to be exceeded.

Temperature of the fuel cladding

- The computed surface temperature of the fuel cladding shall not exceed 125 degrees Celsius under the normal operational or anticipated transient conditions.

Burn-up of the fuel

- The average burn-up of any fuel element or control rod follower shall not exceed 80% of ^{235}U content when fresh.

Reactivity control of the reactor

- The maximum excess reactivity of the core shall not exceed 95% of the total negative reactivity worth of the remaining four control rods, when the two control rods with the greatest worth are fully withdrawn. The maximum positive reactivity worth of movable experiments shall be taken into account when determining the excess reactivity worth.

- The total reactivity worth of all control rods shall not be less than 20 dollars and the worth of any single control rod shall not be less than 2 dollars.

In taking into account two key parameters related to fuel management these are: the reactivity margins and the limitation of the power peaking factor. Where the fuel management strategy leads to an increase in the beginning-of-cycle (BOC) reactivity, it will be important to evaluate the compliance of the core to reactivity margins [10].

The number of fresh fuel assemblies loaded at each reload will have an impact on the BOC reactivity [10]. This parameter also influences whether the reactor is able to meet the required cycle length.

2.4 An in-core fuel management plan

The fuel management plan used for placing fuel assemblies and control rods in the core for each reload was undertaken as described below.

2.4.1 At the beginning of each cycle, three fresh fuel assemblies are loaded into the reactor core generally (but see point 2.4.3 below). This reload is based on the experience that has been accumulated over the years for the efficient operation of SAFARI-1.

2.4.2 The locations that are selected, however, are based on loading the highest masses in the low flux positions. The loading takes place in H3, H7 and B7, which are on the periphery of the reactor core (see Figure 2.1).

2.4.3 An additional criterion for the BOC mass of the core that is applied is that the BOC mass should be approximately 6700 g ^{235}U. If the total mass is higher than the 6700 g, it may be necessary to load only two fresh fuel elements.

2.4.4 When the mass of the fuel assembly is less than 120 g ^{235}U it should be discharged from the reactor core as spent fuel.

2.4.5 Control rods are also replaced based on low ^{235}U mass. When the mass of the most depleted control rod is about 75 g ^{235}U, it and the second most depleted rod are removed from the core, and two fresh control rods are loaded in the subsequent cycle. The loading positions for the two new fresh control rods shall be C7 and G7.

2.4.6 When fresh control rods are loaded, the remaining rods are placed in core positions C5, E7, G5 and E5 in order of highest to lowest ^{235}U mass.

2.4.7 At each reload, load irradiation rigs containing fresh Mo target plates into the six irradiation positions C3, E3, G3, B8, D8 and F8 and leave them for the entire cycle. This modelling approach closely simulates the reactivity contribution of target plates

loaded according to the real irradiation schedule. This issue was confirmed in the dissertation, "Improvement and Validation of OSCAR-3 Usage in SAFARI-1 Core Modelling," [21].

2.4.8 An operating cycle length of thirty days is simulated with a 5-day shutdown period, in accordance with the current operating programme of SAFARI-1.

2.4.9 For modelling purposes, the assumption is made that the core operates at a constant power level of 20 MW. This closely reflects the actual operational conditions of the core.

2.4.10 The most realistic k_{eff} to use in the reactor code computation will be 0.970356 (derived from operational reactor data). This k_{eff} value is a representative value for criticality used when running the OSCAR-3 code taking into account the cycle length and accompanying historical data.

2.4.11 The mass distribution of the reference core is based on operational experience, and serves as a point of departure for the design of the alternative core designs.

2.4.12 The maximum power peaking factor allowed is 3.5. This has also been established in terms of the coupling of the reactor neutronics and thermal-hydraulics, to ensure that the thermal limitations of the reactor are complied with over the duration of operation of the core for a particular configuration.

2.4.13 When considering a new configuration, selected partially burnt elements that have ^{235}U masses between 120 g and 140 g can be placed at the centre of the core in the region of the regulating rod. From evaluation of the core it can be observed that this central region is the location for fuel assemblies of this mass range.

2.4.14 The core configuration that is reloaded in terms of the above in-core fuel management plan is provided below.

Figure 2.1 The SAFARI-1 core configuration for the reference core

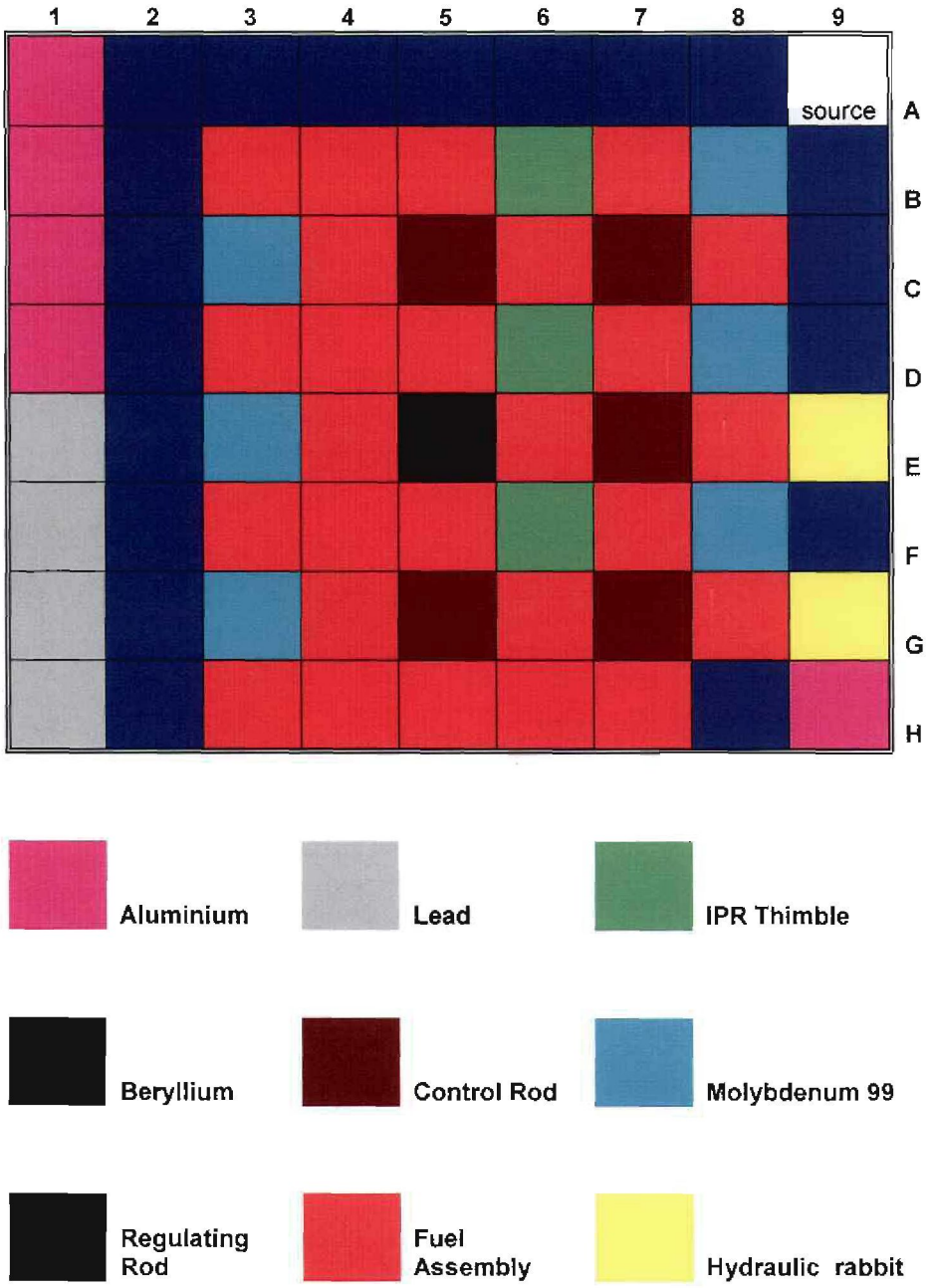

2.4.15 The loading pattern that is used when loading the core configuration in Figure 2.1 is provided in Table 2.3. Fuel assemblies are loaded in such a manner that the highest mass is loaded in B7 and the lowest mass in D5. The mass distribution from the

highest mass to the lowest mass is linear and evenly spread in order to create a uniform flux profile in the core.

Table 2.3 Loading sequence for the core in Figure 2.1

B7⇒H3⇒H7⇒G8⇒C8⇒B3					
1	2	3	4	5	6
B3⇒H4⇒H6⇒H5⇒E8⇒B4					
6	7	8	9	10	11
B4⇒B5⇒D7⇒G4⇒C6⇒C4					
11	12	13	14	15	16
C4⇒D3⇒F7⇒F3⇒D4⇒G6					
16	17	18	19	20	21
G6⇒E4⇒F4⇒E6⇒F5⇒D5					
21	22	23	24	25	26

2.5 Fuel Specification

The fuel specification for the fuel that is utilized in the reactor core is given in Table 2.4 below.

Table 2.4 HEU fuel specifications

Parameter	Unit	Value
Enrichment	% ^{235}U	89 – 93 %
Uranium (^{235}U) meat density in the fuel plate	g/cm^3	3.6089
No. of fuel plates	Quantity	19
Meat length	Mm	606.4
Meat width	Mm	62.5
Plate thickness	Mm	1.20
^{235}U per plate	Gram	15.49
Total ^{235}U	Gram	300.00
Cladding thickness	Mm	0.305
Water gap	Mm	2.7

2.6 Core Configurations under investigation

The core configurations that will be investigated makes provision for the placement of additional nearly spent fuel assemblies in the reactor core. The core configuration is depicted in Figure 2.2. In this core configuration, fuel positions have been added to B9, D9, and F9. There is no reflector material on the west side. An additional location has been made available in position C9 for a hydraulic rabbit. The additional assemblies can be placed either in the western reflector region of the new core or in the central region of the core. The purpose of this operational strategy is to deplete a growing quantity of fuel assemblies with masses between 120 g and 140 g ^{235}U. By depleting these low mass fuel assemblies improved utilization of high-value highly enriched uranium (HEU) will be achieved.

The mass distribution of this core should give rise to the desired performance level providing the required thermal fluxes in the molybdenum production and in the hydraulic rabbit positions.

The essence of this investigation is to compare these two configurations with respect to the reference core. The first fuel arrangement, which is identified as Core B, is characterised by the placement of the nearly spent fuel on the periphery of the core, in positions B9, D9 and F9. In the second arrangement (Core A) these fuel assemblies are placed in the central region of the core, while fresher assemblies occupy the new peripheral positions, following the approach applied in the reference core. Both cores will be subjected to a detailed neutronic evaluation in the results chapter of this dissertation. The core that is selected will need to satisfy the present operational objectives of SAFARI-1 and yield an acceptable power peaking factor that can be used in the safety analysis of the research reactor core.

The mass distribution of Core A was devised by firstly assessing the placement of fuel assemblies in the reference core. It was observed that if one draws three imaginary lines both horizontally and vertically across the core, the outlying regions have heavier masses, while the inner lying regions have fuel assemblies with lighter masses. When devising the placement of masses for Core A this pattern was replicated. For core B, the existing mass distribution of the reference core was retained while the nearly spent fuel assemblies were placed at the outer peripheral locations of the core.

Figure 2.2 Proposed SAFARI-1 core configuration

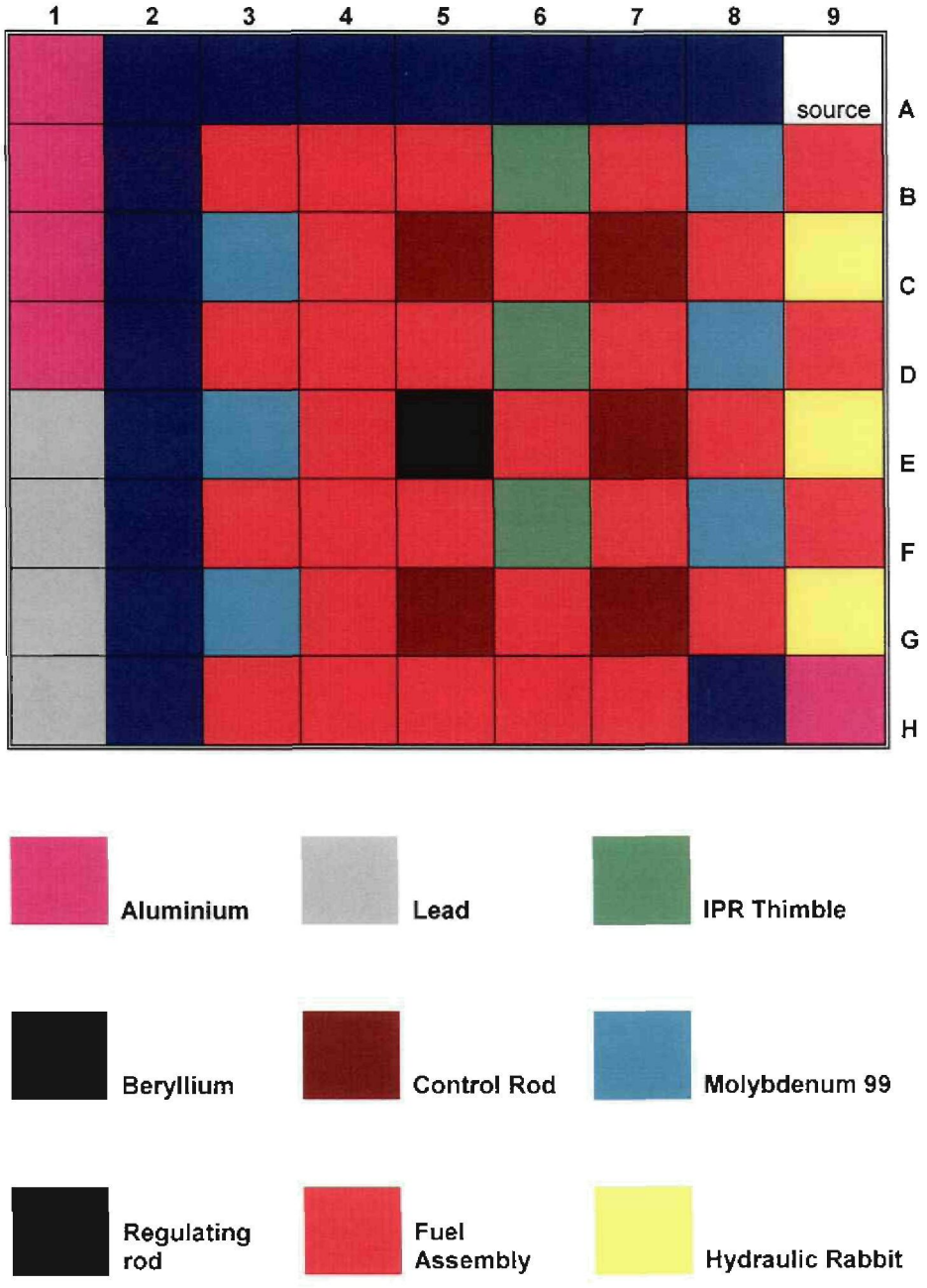

CHAPTER 3 THEORETICAL BACKGROUND

3.1 Introduction

This chapter outlines the theory that is necessary for understanding the basis for the characterisation of a core configuration that must be analysed. The concepts that are discussed are significant for selecting an appropriate core. In the area of fuel management there is a complex relation between various core parameters during the operation of the reactor. The behaviour of neutrons must be adequately assessed in order to arrive at a core that is feasible both technically and economically. A uniform power distribution in the reactor core is essentially ideal for acceptable operation. This factor involves ensuring that depletion is optimal while reactivity control of the reactor core is maintained. The power distribution, depletion analysis, equilibrium conditions, fuel loading, and reactivity control are therefore given consideration within the context of investigating an appropriate core configuration.

3.2 Equation for describing the neutron distribution in the core

For the purposes of the problem under investigation, the physical distribution of neutrons in a research reactor core is described by the multi-group diffusion equation defined in a rectangular spatial region V [20]:

$$-\nabla \cdot D_g(\vec{r})\nabla\phi_g(\vec{r}) + \sigma_r^g(\vec{r})\phi_g(\vec{r})$$

$$= \sum_{h=1}^{G} \sigma_{s0}^{h\to g}(\vec{r})\phi_h(\vec{r}) + \frac{\chi_g}{k}\sum_{h=1}^{G} \nu\sigma_f^h\phi_h(\vec{r}) \qquad 3.1$$

where:

$\phi_g(\vec{r})$ ≡ neutron flux for energy group g.

$\sigma_r^g(\vec{r})$ ≡ microscopic removal cross-section.

$\sigma_{s0}^{h\to g}(\vec{r})$ ≡ microscopic scattering cross-section from energy group h to g.

$\phi_h(\vec{r})$ ≡ neutron flux for energy group h.

$\sigma_f^h(\vec{r})$ ≡ microscopic fission cross-section for energy group h.

χ_g ≡ fission spectrum for energy group g.

ν ≡ average number of neutrons released per fission.

The system is divided into rectangular sub-volumes (or nodes), ΔV, assuming that material parameters are constant within each node. Integrating this over volume and dividing by ΔV we obtain the in-group balance equation for node n and energy group g, which can be written as [20]:

$$\sum_{j=1}^{2M} \frac{1}{h_n^{nj}} \bar{J}_{nj}^g + \sigma_{r,n}^g \bar{\phi}_n^g = \sum_{h=1,h\neq g}^{G} \sigma_{s0,n}^{h\to g} \bar{\phi}_n^h + \frac{\chi_g}{k} \sum_{h=1}^{G} \nu\sigma_{f,n}^g \bar{\phi}_n^h \qquad 3.2$$

where M is the number of spatial dimensions and we define

$\bar{\phi}_n^g$ = average flux in node n

$\bar{J}_{nj}^g$ = average net current from node n to node j

$\sigma_{r,n}^g$ ≡ microscopic removal cross-section in node n.

$\sigma_{s0,n}^{h\to g}$ ≡ microscopic scattering cross-section from energy group h to g.

$\sigma_{f,n}^g$ ≡ microscopic fission cross-section in node n.

In the analytic nodal method, the auxiliary one-dimensional equation in a given direction is solved using analytic methods. The only approximation that this introduces is the one that has assumed the leakage shape [20].

The mathematical method used for solving the equation that describes the distribution of neutrons in the SAFARI-1 research reactor core is the Analytical Nodal Method. In solving for neutronic parameters in OSCAR-3 this method is selected in order to perform the required neutronic analysis for each core configuration.

Nodal methods are fast and accurate, combining attractive features of the finite element method as well as the finite difference method. The unknown function is approximated over a given coarse mesh by a piece-wise continuous function, usually a polynomial [18].

Nodal diffusion methods, which are successful in power reactor analysis, were however regarded unsuitable for research reactor calculations, the reason being that the core is heterogeneous and small, resulting in high leakages, which could invalidate diffusion theory. It has, however, been demonstrated that that such a code system can be successfully used to support research reactor neutronic analysis [14].

Modern nodal diffusion methods, combined with advanced homogenisation and flux reconstruction techniques, have been applied successfully to light water reactor analysis in the last two decades. More recent methods are characterized by the systematic derivation of the relationship between the flux inside the node and the current on its surface [4].

Modern nodal methods share three common features [4]:

(i) The unknowns are defined in terms of the volume-averaged fluxes and/or surface-averaged partial or net currents.
(ii) The node fluxes and surface currents are related through auxiliary one-dimensional equations, obtained by integrating the multidimensional diffusion equation over coordinate directions transverse to the one under consideration.
(iii) The transverse leakage term that appears in the auxiliary equations is approximated by a polynomial (typically quadratic) fit over consecutive nodes.

Nodal methods offer many advantages in computational requirements, which make routine core analysis for research reactors a reality. The suitability of nodal methods for application to MTR core analysis is established. The nodal approach offers considerable advantages over

the standard finite-difference approach and meets the accuracy requirements for core analysis of a research reactor [6].

3.2 Core power distribution

A central component of reactor performance analysis consists of a group of calculational modules that simulate the static neutronic behaviour in the reactor core. The static calculations usually used are based on the solution of the multi-group diffusion equations for the multiplication eigenvalue k_{eff} and the multi-group fluxes characterising the particular core configuration. By calculating the local fission rate, one can construct the corresponding spatial power distribution. The calculation of the core multiplication plays an important role for the determination of the fuel loading and the control of reactivity. The power distribution is an essential input for the subsequent thermal-hydraulic analysis of the core. The nuclear hot channel factors and axial power profile determine how closely the core approaches thermal design limitations and restrictions [1].

The calculation of the core power distribution is the most common type of core analysis performed. The core power distribution is of central importance to fuel depletion studies and thermal analysis. It is desirable to have a core configuration that will result in a flat radial and axial power distribution throughout the core life. In conjunction, the core should have sufficient reactivity to yield adequate fuel burnup while maintaining reactor control during the operating cycle. The calculation of core power distribution will depend on the core enrichment, the location and types of reactivity control, the core geometry and the fuel element design. The determination of the power distribution is also undertaken in order to ensure that all the fuel in the reactor will operate at power densities that are well below conditions that would lead to fuel failure. The power sharing between fuel assemblies is a matter of concern, which can be changed by altering the arrangement of the fuel [1].

The peak-to-average power density, described in terms of a power-peaking factor, is a parameter of the greatest interest as it provides an indication of the upper bound of the thermal properties of the core for a given configuration [1].

Power peaking should be minimised as best as possible within the thermal constraints of the core configuration. The maximum power peaking factor is used as a screening criterion in the selection of suitable cores.

During the process of evaluating different configurations, special attention must be given to ensuring that each core eventually recommended for use by SAFARI-1 has as uniform a power distribution as possible, in order to avoid excessive power peaking. The selection of fuel assemblies with a suitable fissile mass distribution is an important factor in this regard. It is also important that the fuel assemblies should burn evenly in the core during operation. This objective not only ensures safe cores but also cores that operate economically. The combination of accumulated expertise in fuel loading and use of a fuel management code will assist in this exercise.

3.3 Fuel temperature limit

The condition applied at SAFARI-1 to provide an indication of the failure in heat transfer under normal operating conditions is the Onset of Nucleate Boiling (ONB). [13]. In the safety analyses of SAFARI-1 preference is given to using ONB rather than Departure from Nucleate Boiling (DNB), as an indicator for the efficiency of heat transfer under normal operation. At ONB, the fuel surface temperature can be calculated more reliably and is a more useful limit for the fuel cladding calculation.

According to the safety analysis report, the peak fuel clad temperature shall be computed for each newly refuelled core, using core specific measured or computed power density peaks. The resulting peak clad temperature must not exceed 125 °C under normal operating conditions [13].

The calculation of peak fuel clad temperate shall be carried out as follows:

The heat transfer coefficient from the cladding surface to the coolant in fuel channel x is calculated using [13]. This equation is empirical and has been developed for use by SAFARI-1. It is also derived from the Dittus-Boelter equation [17].

$$h_x = 1150\left[1{,}352 + 0{,}0198\frac{(To_x + Ti_{x)}}{2}\right] \times V^{0,8} \times D^{-0,2} \qquad 3.3$$

The numerical values in the expression given in 3.3 represent values used for the determination of the heat transfer coefficient correlation specific to the fuel geometry of the SAFARI-1 research reactor [13].

h_x = The heat transfer coefficient in fuel channel x in units of $W/m^2.K$

$To_x = Ti_x + \Delta T$ is the outlet temperature of channel x.

Ti_x = is the same for all channels and equals the maximum core inlet temperature, Ti_{max}, in °C. $(Ti_{max} = To_{max} - 0{,}0010131 \times \frac{P_{max}}{Q_{min}} = 42\,°C)$

D = is the equivalent hydraulic diameter of the coolant channel in m.

V = is the water velocity in m/s, determined as follows (the extent to which heat is transferred to a moving fluid is also dependent on the velocity [17]):

$$V = \frac{0{,}82 \times Q_{min}}{((0{,}00372 \times N_{fe} + 0{,}00296 \times N_{cr}) \times 3600)} \qquad 3.4$$

N_{fe} = the number of fuel elements

N_{dr} = the number of control rods

The fuel cladding surface temperature in fuel channel x may then be calculated as

$$T_{surface} = Ti_x + \Delta T_x + \frac{0{,}9 \times F_{hs} \times F_{nx} \times W}{0{,}0754 \times h_x} \qquad 3.5$$

0,9 allows for 10% of the total heat that is not transferred through the fuel plate surfaces

Ti_x = is the coolant inlet temperature to channel x in °C

ΔT_x = is the coolant temperature rise in channel x in °C

F_{hs} = is the engineering hot spot/channel factor (use 1,34)

F_{nx} = is the axial neutronic power peaking factor in channel in x.

0,0754 is the heat transfer area through both sides of one fuel plate

W is the mean power in watts generated in one plate, which is obtained as follows:

$$W = P_{\max} \times 10^6 / (19 \times N_{fe} + 15 \times N_{cr}) \qquad 3.6$$

The maximum of all $T_{surface\ clad}$ shall be the peak fuel cladding temperature.

During the operation of the reactor, at some point intersecting the axial and radial plane, the fuel temperature will be at its maximum. It is essential to know what this point is in the reactor and ensure that at this point the fuel cladding temperature does not exceed the thermal properties of the fuel for acceptable operation. For the different configurations that are proposed the fuel cladding temperature must then be calculated so that the operator is confident that the core integrity is maintained throughout the cycle. The methodology described above is used to ensure that the fuel operates within its specified temperature constraint.

3.4 Depletion analysis

During the depletion process, the fuel composition changes because of loss of fissionable material due to fission, build-up and decay of fission products, and transmutation of other reactor materials due to neutron capture. These composition changes occur over a relatively long period of time [2].

Three aspects of depletion analysis are particularly important [2]:

1. The reactivity loss rate associated with fuel depletion.
2. The changes in power distribution associated with depletion, including the effects of control adjustment to maintain criticality.
3. The isotopic transmutation of material that has the greatest economic value linked to fuel cycle costs.

The effects of depletion are simulated using OSCAR-3 by subdividing the time the fuel resides in the reactor into suitable burn-up increments. A depletion analysis is then carried

out for each increment, assuming separability in space and time. The first step in the calculation is the determination of the converged flux for the spatial composition that exists at the beginning of the burnup step. This may include adjustment of control positions to yield a critical eigenvalue. The burn-up step length is chosen to be small enough so that the change in power distribution over the depletion interval is small. The power distribution is then assumed constant over the burnup step. The fission rate during the time step is used to evaluate the change in fuel composition in each spatial region in the reactor. The process is then repeated until the reactor is sub-critical with the control rods withdrawn [2].

In the computations performed with OSCAR-3 a 30-day cycle is simulated in accordance with the burnup steps shown below in Table 3.1.

Table 3.1 Burnup steps for a 30-day operating cycle

Case number	**Type of burnup**	**Number of days**
1	Pure flux	-
2	Depletion	1
3	Depletion	2
4	Depletion	3
5	Depletion	3
6	Depletion	3
7	Depletion	3
8	Depletion	3
9	Depletion	3
10	Depletion	3
11	Depletion	3
12	Depletion	2
13	Depletion	1

Each depletion step is automatically preceded by a flux distribution calculation based on the isotopic inventory and core conditions resulting from the previous depletion. The power density at the core periphery is normally less than the average core power density, yielding a lower depletion rate in these regions. This non-uniform depletion rate causes a redistribution of neutron multiplication in the core during the operating cycle. As a result, the power density near the core periphery tends to increase relative to the average core power density as depletion proceeds, unless there is a compensatory removal of control material from the central region of the core. If such a shift in power distribution occurs, it leads to a greater neutron leakage fraction and as a consequence, a reactivity reduction [2].

During power operation all the materials of which the reactor is composed are subject to change by neutron interaction. The basic equation that describes depletion of isotopes by transmutation and radioactive decay is as follows [2]:

$$\frac{dN^i}{dt} = \lambda^j N^j + \sigma_c^k \phi N^k + y^i \sum_f \phi - \lambda^i N^i - \sigma_a^i \phi N^i \qquad 3.7$$

The time rate of change of the concentration of isotope i in Equation 3.7 is based on three production modes and two loss modes. The production modes are as follows [2]:

1. The first term represents production by radioactive decay of a precursor species, N^j, with a decay constant, λ^j. The production of a given isotope can be by more than one type of decay. As an example ^{238}Pu can be produced by alpha decay of ^{242}Cm or by beta decay of ^{238}Np.
2. The second term represents production by neutron interaction in a precursor species N^k by neutron capture with a spectrum-averaged microscopic cross section σ_c^k. There may also be more than one precursor species for production of a given isotope by neutron interaction. For example, ^{237}U is produced as a result of an (n,γ) reaction in ^{236}U, and also by a (n, 2n) reaction in ^{238}U.
3. The third term in Equation 3-7 represents the production term for fission products, where the value of the fission product yield, y^i, dependents on both the fissioning isotope and the energy of the neutron causing the fission.

The two modes by which the concentration of the isotope i is decreased are [2]:

4. If isotope i is radioactive, it can be lost by radioactive decay with the decay constant λ_i.
5. The final term in Equation 3.7 represents loss by neutron absorption, with a spectrum-averaged microscopic cross section σ_a^i, including fission and capture.

Core depletion calculations using OSCAR-3 are simulated by the quasi-static approach. The flux solution of a static diffusion calculation at a prescribed burn-up step is used for the solution of the time-dependent isotopic depletion calculations, such as Equation 3.7. The microscopic depletion equations are solved analytically, with the flux spectrum and the flux level being kept constant for the duration of the burn-up step [14].

Let us consider a reactor in which the energy from the fission of ^{235}U is released at the rate of P megawatts. With a recoverable energy per fission of 200 MeV, the rate at which fissions occur per day in the entire reactor is, [17],

$$\text{Fission rate} = P(MW) \times \frac{10^6 J}{MW - s} \times \frac{fission}{200 MeV} \times \frac{MeV}{1.6 \times 10^{-13} J} \times \frac{86400 s}{d}$$

$$= 2.7 \times 10^{21} \text{ P fissions per day}$$

To convert this to mass of ^{235}U fissioned per unit time, which is also called the burnup rate, it is merely necessary to divide by Avogadro's number and multiply by 235.0, the gram atomic weight of ^{235}U. This gives

$$\textit{Burn-up rate} = 1.05\ P\ g\ per\ day \qquad 3.8$$

Thus, if the reactor is operating at a power of 1 MW, the ^{235}U undergoes fission at the rate of approximately 1 g/day. In other words, the release of 1 megawatt-day of energy requires the fissioning of 1 g of ^{235}U [17].

The fissile nuclei are, however, consumed both in fission and in radiative capture. Since the total absorption rate is $\sigma_a/\sigma_f = (1+\alpha)$ times the fission rate, it follows from equation 3.8 that ^{235}U is consumed at a rate of

$$\textit{Consumption rate} = 1.05\ (1+\alpha)\ P\ g\ per\ day \qquad 3.9$$

For ^{235}U, the thermal value of α is 0.169 and equation 3.9 shows that this isotope is consumed at the rate of about 1.23 g/day per megawatt of power if the fissions are induced primarily by thermal neutrons [17].

The consumption rate of ^{235}U will be used to estimate the depletion rate of the core in which the partially spent fuel assemblies have been placed in order to ensure that the HEU inventory of SAFARI-1 is utilised more efficiently.

A good understanding of the depletion behaviour of a core is important in terms of effective in-core fuel management. From an operational point of view there will also be a limit on the extent to which fuel can be depleted. If these limits are not adhered to, there could be a risk

of damaging the fuel, possibly resulting in the undesirable release of fission products. The depletion rate of the semi-depleted fuel assemblies to be incorporated into the SAFARI-1 core is an important factor to be considered when evaluating alternative core configurations. Other factors include flux levels, power peaking, and economic operation, while ensuring that the appropriate reactivity control is available.

3.5 The equilibrium cycle

The initial cycle of a reactor core normally consists of entirely fresh fuel assemblies although variations in enrichment and the use of burnable poisons generally mitigate severe power peaking. Fuel assemblies are reloaded in the reactor over a number of cycles. In calculational terms, a core loaded with fresh assemblies is often used as starting point in equilibrium core studies in order to eliminate any bias introduced by a distribution of exposures. Initial cycles are characterised by large start-up perturbations that diminish as successive cores are repetitively loaded according to a fixed strategy until an asymptotic equilibrium is reached. The concept of an equilibrium cycle implies two conditions. First, it implies that operating conditions and constraints, both technical and economic, are invariant from one cycle to the next. Second, it assumes that no unexpected operational disturbances take place that change the cycle energy generation. Although the concept of an equilibrium cycle has value in decision-making, it is seldom achieved in practice. The equilibrium cycle concept is a valuable one in providing a point of reference for evaluating reactor core performance and fuel economy [2].

3.6 Power-peaking effects

Local variations in the neutron flux or power distribution occur in a heterogeneous reactor core configuration. A major concern for the analysis of a particular configuration is the local power peaking that occurs at the boundary between the fuel and the moderator regions. Since the moderator slows down thermal neutrons, one should expect that the fuel elements adjacent to such a water channel would experience a larger thermal flux and subsequently a higher power density. Taking into account that the local flux near the channel may be considerably higher than the average flux in the region, care must be taken not to exceed the thermal limitations of the core. In this regard, it would be important to calculate the local power-peaking factor for the channel that gives rise to the peak-to-average flux [1].

Taking into account the requirement to minimise power peaking in the research reactor core, the maximum power peaking factor is evaluated in order to determine the suitability of a particular mass distribution for the core configurations under consideration. The value of 3.5 is used in the computational code to ensure that the thermal limitations of the core are not exceeded. Cores with values less than 3.5 are accepted as suitable for operational requirements [13].

3.7 Neutron leakage

In order for a reactor to be critical, it is necessary to balance the rate at which neutrons are produced within the reactor with the rate at which they disappear. The neutron economy within the reactor core is affected by neutron leakage. The neutrons that are able to escape from the surface of the reactor do so by leakage. The leakage rate also needs to be balanced with the production rate and the absorption rate within the reactor core, among other reactions. An optimal configuration of the reactor core should result in the neutron leakage being minimised [1].

When comparing the different core configurations under investigation, the configuration that minimises neutron leakage is the most suitable as this would limit reactivity reduction during operation.

A core configuration with less than 30% leakage will be considered acceptable for normal operation. The value of 30% is used based on expert experience with OSCAR-3.

3.8 The multiplication factor

In order to sustain a stable fission chain reaction it is necessary for the fission neutrons from one fission reaction to induce further fission reactions. The reactor core however, should be configured in such a way that a balance is achieved between fission reactions, neutron capture, and leakage. Suppose that one could measure the number of neutrons in two successive neutron generations. One could then define the ratio of these numbers as the multiplication factor k, characterising the chain reaction [1].

$$k \equiv \frac{\text{Number of neutrons in one generation}}{\text{Number of neutrons in preceding generation}} \qquad 3.10$$

For		
	$k = 1$	the reactor is critical
	$k > 1$	the reactor is supercritical
	$k < 1$	the reactor is sub-critical

3.9 Reactivity control

A reactor must be initially loaded with a significantly larger amount of fuel than is required merely to achieve criticality, since the intrinsic multiplication of the core will change during core operation due to processes such as fuel burn-up and fission product production. Sufficient excess reactivity must also be provided to compensate for negative reactivity feedback effects such as those represented by the temperature and power defects of reactivity. The required full power operation that is determined to build up sufficient excess reactivity for a predetermined cycle length depends on the fuel loading and enrichment of the fuel assemblies [1].

To compensate for this excess reactivity, it is necessary to introduce an amount of negative reactivity into the core so that appropriate control of the reactor operation can be applied. This control should be used for the control of power level and if need be, shut the reactor down. The control of reactivity is most often present in the form of strong neutron absorbers. Furthermore, the control reactivity and the apportionment thereof, is a very important aspect of the assessment of core performance and design, understandably having safety implications [1].

An analysis must also be performed to determine the amount of negative reactivity and control required to compensate for the initial excess reactivity contained in the initial fuel loading [1].

Reactivity control can be further characterised by some useful definitions [1].

(1) Excess reactivity ρ_{ex}: The core reactivity present with all the control rods withdrawn from the core. The excess reactivity will be a function of both time and temperature.

(2) Shutdown margin ρ_{sm}: The negative reactivity of the core present when all control rods have been fully inserted to achieve minimum core multiplication. The shutdown margin is also a function of time and temperature.

(3) The total control rod element worth $\Delta\rho$: The difference between the excess reactivity and the minimum reactivity when all control rods are fully inserted.

$$\Delta\rho = \rho_{ex} + \rho_{sm} \qquad 3.11$$

Operational limits and conditions for reactivity control are specified in the Safety Analysis Report of SAFARI-1 [13]. The core configurations that are investigated need to comply with these limits and conditions.

3.10 Fuel loading variables and constraints

At the beginning of each reload cycle the fuel loading variables that are normally available are the number of fresh fuel assemblies to be loaded, the loading pattern, partially burnt fuel assemblies that will be reinserted, and measures used to control the excess reactivity of the reactor during the cycle [2].

The selection of a fuel-loading plan is subject to certain constraints. The first involves the number of fuel assemblies that will be loaded in the core at beginning-of-cycle. In the case of SAFARI-1 the number of fuel assemblies that can be loaded in any single core is 26 to 31 fuel assemblies [13].

The discharge burnup of the fuel is also subject to constraint. Fuel burnup results in a gradual build-up of fission products in the fuel matrix, which results in both fuel swelling and potential gaseous fission product release [2]. Moreover, the accumulation of fission product poisons and the depletion of fissile material reduce the reactivity of a fuel assembly and hence its contribution to the criticality of the core.

An additional constraint is the capacity of the reactivity control arrangements for the reactor core. If cycle energies are large, the excess reactivity to compensate for the effects of fuel depletion must also be adequate. The control limit then impacts on the amount of excess reactivity that can be accommodated at beginning-of-cycle [2].

The following safety and technical constraints are applicable to the problem under investigation as indicated in Table 3.2.

Table 3.2 Constraints for the core configurations

Constraint	**Variable**
Safety constraints	Power peaking factor ≤ 3.5
	k_{eff}=0.970356
Technical constraints	Cladding temperature ≤ 125 ° C
	Number of fuel assemblies: 26 to 31
	Number of control rods: 6
	Total control rod worth not less than 20 dollar

For each core configuration that is proposed in this investigation, the core will comply with these constraints that have been specified in the above table. Besides being linked to the safety envelope within which the core operates, these constraints are also determined by the design limitation of the core. For cores of similar external geometry and material specifications, the constraints remain unchanged. When there is a significant change in the geometry and design of the core, it would be expected that the thermal limitation of the core be re-evaluated so that core integrity can be maintained during operation.

3.11 The fuel arrangement

A determination of the fuel arrangement that best satisfies the power distribution, operational objectives and constraints of the reactor core is an extremely complex problem. Generally, an evaluation of the time-dependent power distribution performance for all possible arrangements is unfeasible even if symmetry is designed about the axes of the core. A common approach adopted for a loading rule is to minimise the fissile inventory on the one hand, and also reduce the power peaking factor below acceptable limits on the other hand [2].

To determine the specific position of each fuel assembly, it may be possible to resort to a direct search algorithm for this step. This would require some form of power distribution evaluation for each possible fuel configuration. A likely solution to this problem is some combination of direct search with an empirical loading rule based on experience or more detailed calculation. This exercise could be the subject of further research that would be beyond the scope of this dissertation [2].

The specific position of each fuel assembly for the purpose of the computational code evaluation is based on experience in operating the SAFARI-1 reactor core. A fissile mass distribution that places heavier assemblies at the periphery of the core (positions of lower neutron flux) and lighter assemblies in the centre of the core (positions of higher neutron flux) has been applied. This fuel arrangement yields a more uniform power distribution and even burnup in the core.

It can be illustrated that a reactor core in which the average infinite multiplication factor in the central region is unity, surrounded by a relatively thin region of higher reactivity, should approach the desired uniform power distribution. This loading scheme is referred to as zonal loading in which one loads unirradiated fuel in the periphery zone of the core and lighter, partially spent fuel towards the centre. The irradiated fuel is then shuffled in toward the inner zone, while the fuel in the central zone is discharged from the core [2].

From the consideration of the possible fuel arrangements that are possible, this determination is a complex mathematical problem that is beyond the scope of this investigation. However, more stepwise changes in the core can be evaluated by heuristic methods. The core that is being proposed combines the use of heuristic methods and the fuel management code functionality.

3.12 Effect of neutron fluence

The fission process occurring in nuclear fuel produces enormous numbers of neutrons of widely differing energies. Much study of the role of neutrons of varying energies has shown that displacement damage (the primary basis for property changes) in metals is produced largely by the higher energy neutrons, hence the convention of describing neutron exposure in neutrons per square centimetre having energies of more than one million electron volts,

abbreviated: $n/cm^2 > 1$ MeV. Experiments have shown that the lower energy neutrons contribute little to the kind of damage that produces changes in toughness called radiation embrittlement. The damaging capacity of high-energy neutrons therefore needs to be measured [15].

This process is a major task and one, which must be undertaken with great assurance of accuracy since the embrittlement of the reactor internals cannot be measured by non-destructive means; hence projections are required. Such projections can be derived from testing of specimens of the reactor internals in situ and from dosimeters at the same position. Extrapolation of these results to the reactor internals is required and this will involve projection of both the neutron fluence and spectrum at the core box wall, coupled with a related embrittlement projection [15].

If one knows the neutron flux and fluence (time-integrated flux), the neutron energy spectrum (distribution by energy level), it is then possible to rate or rank the embrittlement sensitivity of the structural materials and to establish conservative trends [15].

The fluxes and fluences seen by various reactor components will alter the mechanical properties of the components. Radiation effects in aluminium at the temperature of interest are driven primarily by two sources. One is point defects, vacancies, and self-interstitial atoms, created when aluminium atoms are displaced from their lattice positions. The other are precipitates of transmutation-produced silicon. Transmutation products in aluminium are primarily silicon from reactions with thermal neutrons as well as hydrogen and helium generated by fast neutrons [16].

Several factors affect the degree of embrittlement for various structural materials. These include [15]:

(i) Type of material, and its composition and microstructure
(ii) Exposure temperature
(iii) Neutron environment
(iv) Stress state of material
(v) Combined embrittlement effects.

The irradiation limit for SAFARI-1 is paralleled with the Petten research reactor in the Netherlands. The structural material used in these reactors is derived from the 5000 series aluminium alloy. The replacement of the Petten vessel took place in 1986 after it had accumulated to [13]:

7.1×10^{22} n/cm^2, fast neutron fluence, and
7.5×10^{22} n/cm^2, thermal neutron fluence.

By comparison, by 1998, when the energy delivery of SAFARI-1 had accumulated to 1.4×10^6 MWh, the total fluence accumulated at that stage by this section of the core box was [13]:

1.26×10^{22} n/cm^2 fast, and (neutron energies above 0.625 eV)
2.27×10^{22} n/cm^2 thermal. (neutron energies up to 0.625 eV)

The limit that is applied is 6.5×10^{22} n/cm^2 thermal neutron fluence.

3.13 Conclusion

The foregoing theoretical discussion should provide a frame of reference for the problem that is being investigated in this study. The theory also points to the ideal in terms of understanding the basis of selection of a suitable core configuration. It also describes the envelope under which the reactor should be operating in order to satisfy the safety and technical constraints that will be encountered. The results of the investigation will be evaluated using the theory as a backdrop. The essential aspects such as an equilibrium core are pointed out as significant. In addition, the theory is an essential insight for the analysis that is required in this study.

CHAPTER 4 THE CORE-FOLLOW CALCULATIONAL SYSTEM

4.1 Introduction

The investigation into different core configurations for SAFARI-1 was conducted using a core analysis code system. This system, known as OSCAR-3, has been designed for Cartesian geometry type Pressure Water Reactor and Material Test Reactor cores, and was used to quantify the state of the reactor core and the neutron flux levels in the irradiation locations of SAFARI-1. OSCAR is the acronym for "Overall System for the Calculation of Reactors". The code is a multi-group, three-dimensional, advanced nodal diffusion tool with full cross section feedback and depletion capabilities [7].

The OSCAR-3 system is the third version of OSCAR. The initial OSCAR system, OSCAR-1, was developed in the early 80's. OSCAR-1 as well as its extension, OSCAR-2, developed in the late 1980's, were based on traditional finite difference neutronic methods and consisted of several codes that interacted poorly with each other by means of pre-and-post processors. Development on OSCAR-3 started in 1991 with the explicit aim to develop a more integrated package for core analysis based on modern nodal methods developed within Necsa [19].

The design of OSCAR-3 can be viewed as consisting of four sub-systems as depicted in Figure 4.1.

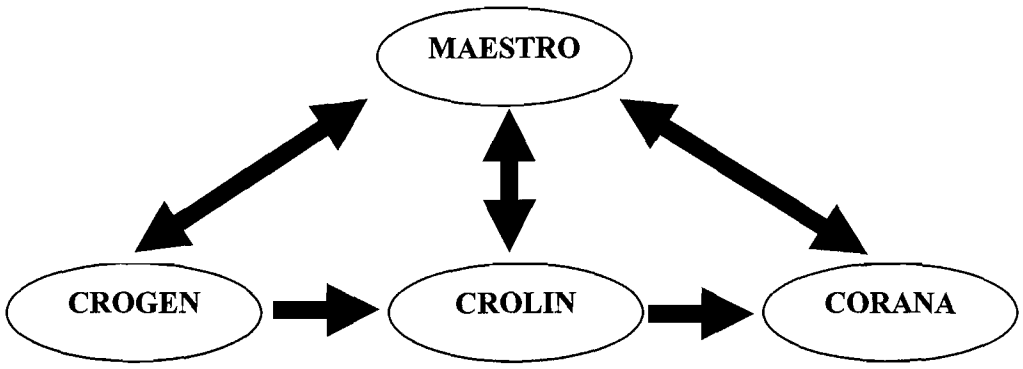

Figure 4.1 Modules of the OSCAR-3 system

The MAESTRO sub-system is the module that takes control of the system integration and execution. The programs available in MAESTRO are the config editor, exposure editor, shuffle, mgrac, results viewer, and report generator [19].

CORANA is the core analysis module. CORANA is an acronym for "CORe ANAlysis". The main code in CORANA is MGRAC, an analytical nodal diffusion code [19].

CROGEN is the cross-section generation system of OSCAR-3. It is an acronym for "CROss section GENeration", and it contains several codes to create few-group cross-section data using various methods. The main code in CROGEN is heade [19].

CROLIN, the cross-section linker, takes outputs from CROGEN calculations and converts them into a common file format that can be used in the core-follow calculations. CROLIN is an acronym for "CROss section LINker" [19].

4.2 MGRAC

MGRAC stands for "Multi-Group Reactor Analysis Code" and is used for the core analyses of the different core configurations in this dissertation. It solves the static neutron diffusion equation in an arbitrary number of energy groups, using either a standard mesh centred finite difference or advanced multi-group analytical nodal method. As indicated in Chapter 3, the method that has been used to characterise the neutron behaviour in the reactor is the advance nodal method [7].

MGRAC incorporates an accurate coarse-mesh method, which is specifically suited for applications to whole assemblies as presented in this dissertation. The whole assemblies have been homogenised in the radial direction. The basic geometry represents a Cartesian array of rectangular channels subdivided into axial layers [7]. The number of energy groups that are used while solving the neutron diffusion equation is six. The energy spectrum for the groups is given in Table 4.1 below, as follows:

Table 4.1 Levels for six energy groups

Energy Group	**Electron volt** (eV)
1	8.21×10^{5}
2	5.53×10^{3}
3	4.0
4	0.625
5	0.14
6	1.1×10^{-4}

MGRAC uses a quasi-static approach to model the long-term behaviour of a reactor core. Static diffusion theory calculations at selected time points determine the flux or power levels used for the solution of the time-dependent isotopic depletion equations over broad time steps, represented by burn-up steps in the code input. For the static neutronic calculations, a cross-section feedback model using a quadratic polynomial library (a LINX file) is incorporated to cater for power and burn-up dependent feedbacks [7].

The flux solution of a static neutron diffusion calculation at a predefined burn-up step is used as input for the solution of the time-dependant isotopic depletion calculations. While the power level is kept constant for the duration of the burn-up step, the microscopic depletion equations are solved analytically. The depletion calculations performed in the nodal and a "re-depletion" model corrects assembly codes. In OSCAR-3 a correction is calculated by repeating the depletion calculation using the homogenised cross-sections and the specific burn-up chains, but using the flux levels and burn-up time steps of the assembly calculation. The macroscopic section is corrected at each burn-up time step by tabulating the difference in number densities [7].

When running the MGRAC code the main variables that are inputted are:

1. Target k_{eff}.
2. Burn-up time steps for every case.
3. From point 2 the operating cycle length (30 days).
4. The power level (20 MW at full power).

The following main options in the code are selected:

1. The standard analytical nodal method option is selected.
2. The rod search option is activated.

4.3 SHUFFLE

SHUFFLE is a fuel shuffling code which is designed for moving assemblies from several sources to a destination by point and click methods. Advanced algorithms allow for the strategic movement of assemblies, and make provision for saving a load strategy for operation of the reactor core. The SHUFFLE Graphical User Interface (SHUFFLE GUI), which is part of the MAESTRO sub-system of OSCAR-3, provides for this interface. The configuration of the core is specified in the SHUFFLE Input File and forms the basis for the core calculation and depletion analysis [19].

The SHUFFLE code was developed for providing a multiple cycle capability to the Multi-Group Reactor Analysis Code (MGRAC). It is designed to be a precursor to the nodal reactor analysis code. It can be used as a pre-and-post processor for a single core cycle. In the SHUFFLE mode assemblies are placed in a specified core-loading pattern. Assemblies are moved to and from the reactor core, vault, and storage pool. Starting with each reload, the initial conditions of each core are obtained by the modelling of out-of-core isotopic decay within a destination core. An initial core is then set up in accordance with the user's specifications. SHUFFLE is therefore a practical device for the assembly of fuel and reflector elements within a core. The basic geometric configuration of a reactor core is portrayed as a Cartesian array of fuel assemblies. The depletion status of all assemblies in a core is saved in an "exposure" file. The file stores data about the core and the type of assemblies [19].

4.4 Application of OSCAR-3

It has been demonstrated that OSCAR-3 can be used for core-follow calculations of the SAFARI-1 research reactor and to investigate the impact of various operational strategies [11].

The core analysis undertaken in this dissertation is therefore considered to be highly accurate and reliable from a calculational point of view.

CHAPTER 5 AN EQUILIBRIUM CORE STUDY

5.1 Foreword to study

An equilibrium core study was performed for the present operating reactor core configuration of SAFARI-1. The fuel element design and core geometry are in accordance with the reference core. The parameters that were evaluated when observing the changes to the reactor core were the control rod bank positions, the BOC mass of the core, the cycle operating length, the thermal fluxes at certain positions and the discharge mass. The simulated changes to the reactor core and the analyses thereof were assessed by means of the OSCAR-3 calculational system. The methodology described in this chapter can be used to obtain an equilibrium core for the different configurations and fuel loading patterns described, taking into account the lessons learnt while doing this exercise. The important operating parameters are given in Table 5.1.

An equilibrium core for a specific core configuration can be obtained by reloading and burning the core repeatedly until equilibrium conditions are reached. When equilibrium conditions are in place the reload pattern and the cycle operating length converge, resulting in the BOC ^{235}U mass distribution being constant after every reload. Equilibrium core calculations may also be performed for different core configurations in order to determine the long-term fuel economy for optimal reactor performance. Equilibrium core studies also determine the most appropriate core layout that will provide high thermal fluxes while operating within an envelope of the safety and fuel constraints of the reactor core.

Table 5.1 The core operating parameters for the equilibrium core study

Parameter	**Value**
Power	20 MW
K_{eff}	1.000
Cycle length	24.625 days
BOC mass of ^{235}U	9168.6 g
Number of fuel assemblies	26

5.2 Fuel loading strategy

A fuel loading strategy was chosen that would be suitable to produce an equilibrium core. The following procedure was followed:

(i) The reactor core was loaded at the start with fresh fuel in all 26 locations of the core. The 300 g ^{235}U fuel assembly and the 200 g ^{235}U control rod was used.

(ii) For every reload, 3 fresh fuel assemblies were loaded into the core for each cycle. The positions of the fresh fuel assemblies were not specified. Fuel assemblies were discharged from the core when the mass burned up to less that 120 g ^{235}U.

(iii) For every reload, a fresh control rod assembly was loaded into position C7 of the core. When the mass of a control rod reached 60 g ^{235}U, it was removed from the core. An independent shuffle pattern was used for the placement of the control rods in positions C7, E7, G7, and, C5, E5, G5.

(iv) Due to the artificially high excess activity for the first 5 cycles, it was necessary to use a target k_{eff} of 1.04. If this value were not used, the control rod search facility of OSCAR-3 would fail to converge. Subsequently, from cycle 5 onwards, a target k_{eff} of 1.00 was used for the core calculation.

(v) At every reload, the STRAT mode of OSCAR-3 was used to reload fresh fuel into the respective open positions in the destination core. The mode that was used was High Mass $\Rightarrow$ Low Flux to populate the core.

(vi) The core was evaluated for equilibrium core conditions at cycle 25. Following this evaluation, fresh fuel was pinned in the core at B3, B7, and H7, and a further 5 cycles were simulated. A scheme was devised for selecting which were the appropriate locations to use for the pinned fuel. This was derived from the analysis of each reload.

5.3 The most likely high-mass fuel assembly locations

The initial parameters that were evaluated after each reload were the control rod positions. The positions of the three heaviest fuel assemblies were recorded. The STRAT mode of the computational code was used for cycle 5 to 25. The table below illustrates how the 3 pinned locations for loading fresh assemblies were determined.

Table 5.2 Analysis of loading locations using STRAT mode

Cycle #	Position 1	Position 2	Position 3	B3	B7	H7
5	F3	E4	D3			
6	H6	H7	G8			X
7	H3	H4	H7			X
8	H6	H7	G8			X
9	B3	B4	B5	X		
10	H6	H7	G8			X
11	B3	B4	B7	X	X	
12	H6	H7	G8			X
13	B3	B4	B7	X	X	
14	H3	H7	G8			X
15	B3	B4	B5	X		
16	H5	H7	G8			X
17	B3	B4	B5	X		
18	H5	H6	H7			X
19	B3	B4	B7	X	X	
20	H3	H7	G8			X
21	B3	B4	B7	X	X	
22	H3	H7	G8			X
23	B3	B4	G7	X		
24	H3	H7	H8			X
25	B3	B4	B7	X	X	

From the above analysis it can be deduced that the most likely locations selected by the STRAT capability of the code were B3, B7, and H7.

5.3 The change in beginning-of-cycle mass

The BOC mass for a cycle is a key parameter that should be observed to assess equilibrium core conditions. A BOC mass of ^{235}U of about 6700 g is a target mass for subsequent cores. For this particular core configuration, it is expected from experience that the core should reach equilibrium in about 25 cycle iterations. As the core approached equilibrium, the change of mass became less pronounced and should essentially be invariant. The BOC mass is considered to be a global parameter for the core.

The change in the BOC mass of each core was recorded for 30 cycles. Table 5.6 denotes the information in regard to the change of BOC mass for 30 cycles. The initial BOC mass noted was 9168.6 g ^{235}U for the first cycle. From cycle 1 to 9, there was a sharp rate of decrease in the BOC mass for the each core. From cycle 10 to 16, the decrease in mass was more gradual. From cycle 17 to 25, the difference in mass was very small after each reload. From cycle 25 to 30, the core had started to exhibit equilibrium core conditions based on the behaviour of this global parameter.

Table 5.6: BOC mass of the reactor core

Cycle	Mass in gram (^{235}U)
1	9168.6
2	8682.3
3	8278.2
4	7951.0
5	7693.3
6	7493.3
7	7348.4
8	7242.3
9	7190.9
10	7139.9
11	7104.5
12	7080.6
13	7063.0
14	7054.1
15	7048.1
16	7043.3
17	7039.2
18	7036.1
19	7032.6
20	7018.0
21	7012.9
22	6996.7
23	6972.6
24	6949.6
25	6945,5
26	6930.3
27	6930.8
28	6922.6
29	6922.8
30	6915.8

5.4 The change in the relative assembly power density at E4

The relative power distribution is considered a local variable since it is determined for each fuel assembly position of the core, and as such a stricter indicator of equilibrium status. The rate of change of this parameter (monitored in core position E4 as an example) was high from cycle 1 to 9. The changes in relative assembly power distribution are given in Table 5.7. From cycle 10 to 16, the parameter was fairly constant. This behaviour seems to be unusual, and given the downward trend in core mass, not indicative of equilibrium. From cycle 18 to 25, there were smaller variations observed for each cycle iteration. The variations from cycle to cycle over this range exhibited oscillations.

Table 5.7 Relative assembly power density at location E4

Cycle	Value
1	1.87
2	1.72
3	1.63
4	1.51
5	1.41
6	1.39
7	1.27
8	1.21
9	1.23
10	1.20
11	1.20
12	1.20
13	1.21
14	1.19
15	1.24
16	1.19
17	1.18
18	1.20
19	1.22
20	1.19
21	1.23
22	1.30
23	1.22
24	1.29
25	1.21
26	1.27
27	1.21
28	1.26
29	1.21
30	1.26

Figure 5.1 depicts the behaviour of this variable graphically, with clear indication of the oscillatory behaviour.

Figure 5.1 The Graph of the relative assembly power density at location E4

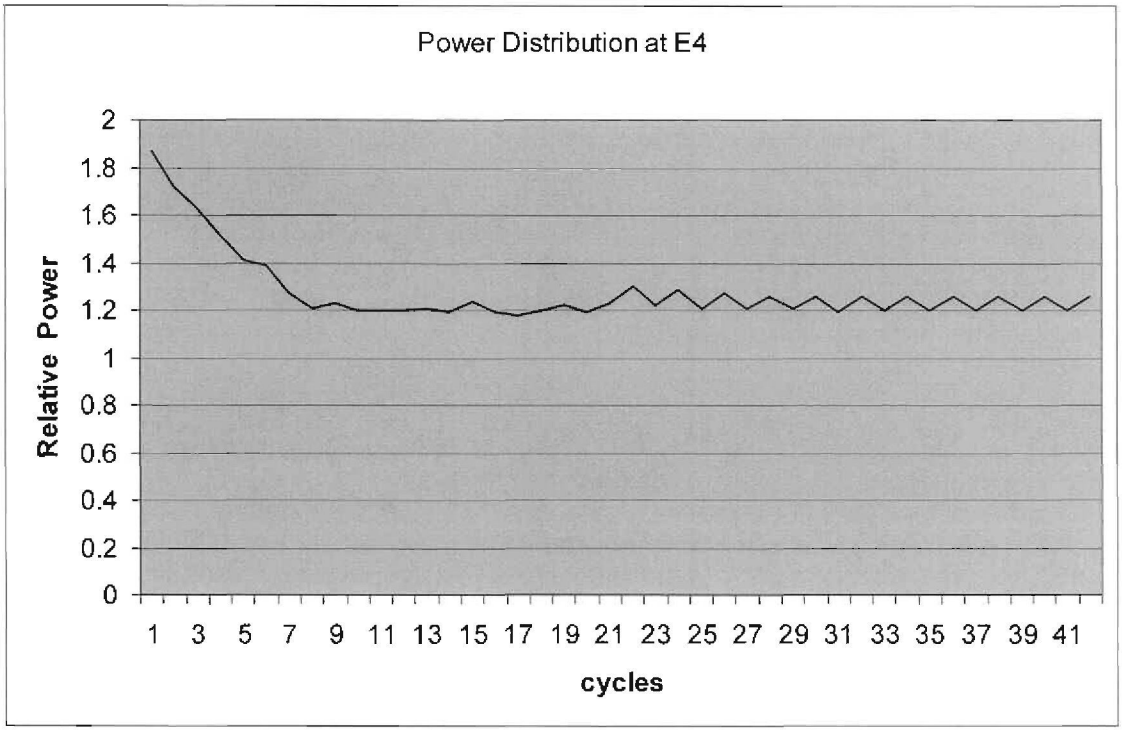

5.5 The change in the mass discharged from the core

The amount of mass discharged from the core after each reload is an indication of the economy of the core. It is desirable to discharge less mass from the core while utilising an optimal mass for the core taking into account the required cycle length. As successive reloads were performed, there was a decrease in the discharge mass. Bearing in mind that this too is a global parameter, there appears to be an approach to equilibrium. Cycles 16 to 25 were selected so that the behaviour of the discharge mass can be observed as the core approaches apparent equilibrium. At equilibrium conditions the discharge mass should be invariant.

Table 5.3 Mass discharged for cycle 16 to 25

Cycle	Mass discharged
16	390.6 g
17	372.1 g
18	373.4 g
19	365.8 g
20	380.8 g
21	372.8 g
22	360.2 g
23	354.9 g
24	341.8 g
25	345.9 g

5.6 The change in the thermal flux at irradiation position G3

The behaviour of the thermal flux was observed at the G3 location. This location is one of nine irradiation locations in the SAFARI-1 core and thus an important indicator of a suitable core configuration. The flux is of the order of magnitude of 10^{14} $n.cm^{-2}.s^{-1}$ and is favourable for isotopic transmutations. Cycles 16 to 25 are again noted. The variations observed in the thermal flux indicate oscillations. In contrast to a global variable such as the BOC mass of the core, this local parameter still is not invariant as ideal equilibrium conditions dictate. However, alternate cycles compare well. This trend is observed even up until cycle 30. The change in thermal flux propagates in sequence in a periodic manner. This parameter demonstrates an equilibrium that occurs periodically.

Table 5.4 Thermal flux from cycle 16 to 25

Cycle	Thermal Flux* $n.cm^{-2}.s^{-1}$
16	1.63×10^{14}
17	3.81×10^{14}
18	2.48×10^{14}
19	1.34×10^{14}
20	2.51×10^{14}
21	1.36×10^{14}
22	2.55×10^{14}
23	1.30×10^{14}
24	2.58×10^{14}
25	1.32×10^{14}

* (for neutron energies up to 0.625 eV)

5.7 Conditions of an equilibrium core

The position that Graves [2] puts forward on equilibrium cores is as follows:

> Although the concept of an equilibrium cycle has value in comparing alternative courses of action, it is seldom achieved in practice. Two conditions need to co-exist in an equilibrium core.
>
> (i) The operating requirements and constraints, both technical and economic, are invariant with time.
>
> (ii) No unexpected operational disturbances should take place that alter the cycle energy generation or the refuelling fraction.

5.8 Change in control rod positions

The BOC control rod positions up until the end-of-cycle (EOC) positions are observed for cycle 20 to 25, as indicated in Table 5.5. These cycles were chosen in order to evaluate the changes as the core approaches equilibrium conditions. The control rod positions were

recorded for every burnup step, and are denoted by the cases given in the table. Within the conditions of high excess reactivity in the core, the control rods at BOC were still deep in the core. At BOC, the control rods are generally inserted beyond the operating limit, indicating that the STRAT scheme employed results in cores that are too heavily loaded. The starting positions for this core configuration are therefore not ideal for actual operating conditions for the SAFARI-1. As the burn-up takes place the control rods are withdrawn from the core; this data should therefore be considered an indication of the changes that occur as the reactor operates through the cycle length At the EOC the control rods are still relatively deep in the core and the actual values are not considered to be ideal for reactor operations. As with the other local parameters of the reactor core, the variability is periodic, comparable to the distributions of thermal flux and, relative power, and for the depleted mass at specific locations in the core. From observation, the control rod positions that show reasonable comparison occur for cycle 20, 22, and 24.

Table 5.5 Control rod positions per burnup step for cycle 20 to 25

Case	20 (notches)	21 (notches)	22 (notches)	23 (notches)	24 (notches)	25 (notches)
1	2616	2255	2613	2038	2577	2040
2	3126	2830	3151	2647	3056	2650
3	3299	3073	3318	2933	3269	2883
4	3342	3182	3359	3132	3318	2936
5	3395	3292	3447	3261	3379	3141
6	3560	3370	3612	3349	3514	3266
7	3681	3513	3722	3451	3656	3353
8	3768	3676	3801	3643	3753	3471
9	3832	3779	3860	3643	3824	3654
10	3952	3853	4040	3760	3931	3770

Figure 5.2 The Graph of the change in BOC mass for 30 cycle iterations

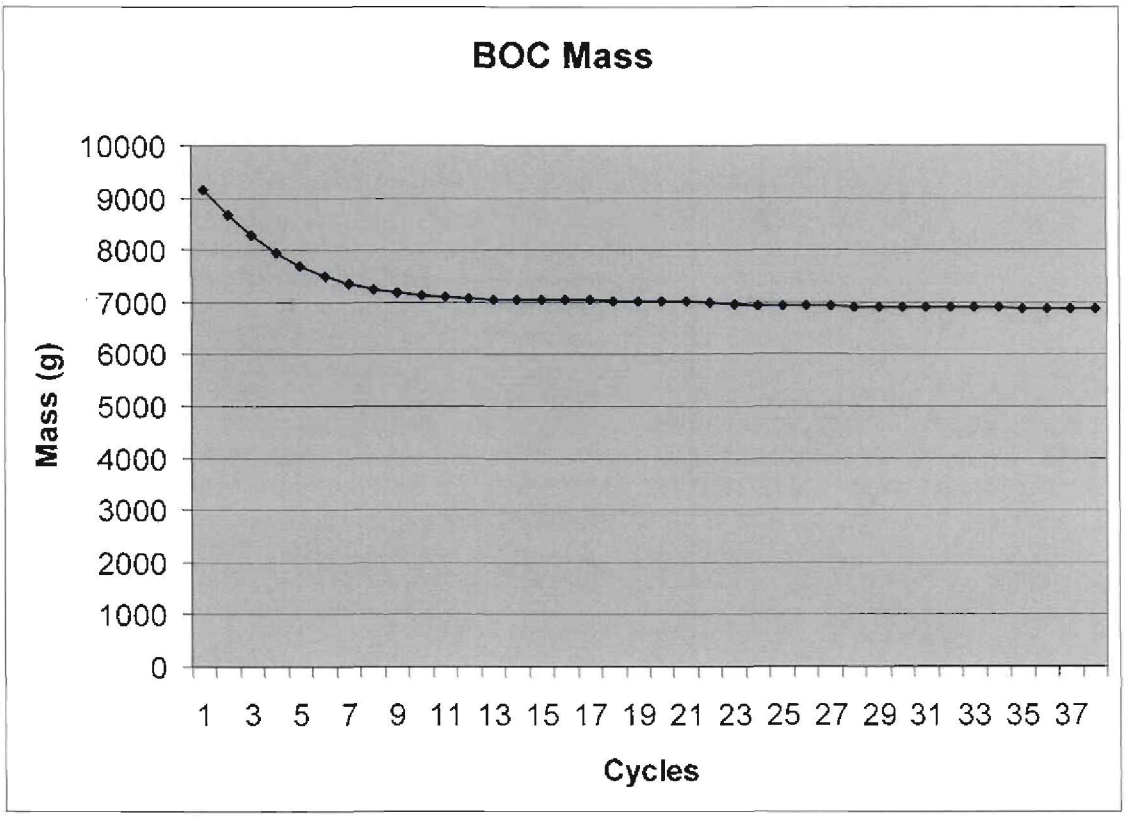

5.9 Conclusion

The exercise to demonstrate that equilibrium can be reached following the proposed fuel loading strategy in Section 5.2 did not result in an ideal equilibrium state for the core. The core exhibited an equilibrium state that oscillated from north to south. When using the STRAT mode in OSCAR-3 (which selects the high-mass to low-flux positions automatically) for the three fuel assemblies, placement was performed by the code alternating between north and south. The effect would be that the flux profile would also change in accordance with this placement behaviour. It was therefore not possible to obtain invariant change in mass at these locations after each reload was done. Variables that also exhibited these oscillations are relative assembly power density and control rod positions. This behaviour was confined to the local reactor core variables. The decision to load three fresh fuel assemblies at each reload contributed to non-equilibrium core conditions In addition, the loading of a fresh control rod for each reload had the same effect. If the intervention of pinning the fresh fuel were implemented earlier than cycle 25, an equilibrium core may have been attainable; however, it implies that the high mass to low flux strategy *per se* is not sufficient for obtaining an equilibrium core. The oscillations produced were therefore due to the fuel loading strategy adopted for this exercise.

CHAPTER 6 RESULTS AND DISCUSSIONS

6.1 Introduction

In this chapter, the results of the neutronic calculations performed on the different core configurations are presented. These results will serve as a basis for providing a proposed solution to the problem statement that has been set out in this dissertation. The generation of an equilibrium core as performed in the previous chapter is an essential process that must be undertaken before a particular core configuration can be analysed. When sufficient reloads of a core have been performed and the local and global core parameters have reached equilibrium the neutronic analysis can then be performed. The results that are obtained from the cores in this chapter should be determined from equilibrium core hence the significance of the exercise in Chapter 5. The core configurations in this chapter exhibit equilibrium characteristics that validate the neutronic analysis that has been undertaken.

6.2 Fissile mass distribution

The fissile mass distribution is denoted in Figure 6.1 for the reference core of SAFARI-1. This core operated for a 30-day cycle at a constant power of 20 MW with a k-effective of 0.969181. The maximum power-peaking factor for this core is 2.92. This value falls within the constraint of being less than 3.5.

The fissile mass distribution for Core A is depicted in Figure 6.2, and presented in tabular form in Table 6.1. It is evident that the masses are distributed in a linear manner from the lowest mass to the highest mass. The proposed locations for the 3 fuel assemblies that vary in mass between 120 and 140 g ^{235}U are as follows:

D5
E4
F5

These positions are located around the regulating rod of the reactor core.
The positions for Core B are:

B9
D9
F9

and the fissile mass distribution in this case is illustrated in Figure 6.3.

Figure 6.1 The fissile mass distribution of the reference core

Fissile mass distribution (g of ^{235}U): Reference core

Al	Be	Be	Be	Be	Be	Be	Be	**source**
Al	Be	**264.43**	**227.60**	**220.56**	**IPR**	**300.00**	**IPR/Mo**	**Be**
Al	Be	**Mo**	**199.13**	**167.36**	**202.41**	**199.15**	**271.63**	**Be**
Al	Be	**191.67**	**167.18**	**132.00**	**IPR**	**216.46**	**Mo**	**Be**
Pb	Be	**Mo**	**148.42**	**108.17**	**144.10**	**164.21**	**235.87**	**Hydr**
Pb	Be	**168.43**	**147.76**	**133.73**	**IPR**	**176.87**	**Mo**	**Be**
Pb	Be	**Mo**	**209.20**	**108.84**	**153.18**	**199.15**	**277.91**	**Hydr**
Pb	Be	**300.00**	**251.53**	**249.81**	**250.45**	**278.69**	**Be**	**Al**

Al	Aluminium	k-effective	0.969181	
Be	Beryllium reflector			
Hydr	Hydraulic rabbit	BOC Mass	6639.4	g of U-235
Mo	Molybdenum-99			
Pb	Lead	Power-peaking	2.92	
IPR	Irradiation Rig			
	Regulator rod			
	Control rod			

Figure 6.2 The fissile mass distribution (g of ^{235}U) of core with nearly depleted masses in the central region of the core: Core A

Fissile mass distribution: Core with depleted assemblies in central region

Al	Be	Be	Be	Be	Be	Be	Be	source
Al	Be	255.72	235.83	228.75	IPR	277.07	Mo	300.01
Al	Be	Mo	160.66	147.06	235.83	199.15	255.78	Hydr
Al	Be	157.04	151.47	125.11	IPR	218.81	Mo	257.01
Pb	Be	Mo	131.76	113.11	151.47	146.36	250.51	Hydr
Pb	Be	154.94	142.36	129.90	IPR	154.94	Mo	285.48
Pb	Be	Mo	170.52	115.49	146.83	199.15	266.22	Hydr
Pb	Be	300.01	278.47	255.22	257.01	300.01	Be	Al

BOC	Mass	7232.60
PPF		3.36
keff		0.969180

PPF: power-peaking factor

Table 6.1 The mass distribution of Core A for the lowest mass to highest mass

Location in core	Value in gram ^{235}U
D5	125.11
F5	129.90
E6	130.15
E4	131.76
F4	142.36
G6	146.83
D4	151.47
F3	154.85
F7	154.94
D3	157.04
C4	160.66
C6	167.14
G4	170.52
D7	218.81
B5	228.75
B4	235.83
E8	250.51
H5	253.27
H6	253.75
B3	255.22
C8	255.72
D9	257.01
G8	266.22
B7	277.07
H4	278.47
F9	285.48
B9	300.00
H7	300.00
H3	300.00

The fissile mass distributions for 7 cores are provided in Appendix A. These 7 cores were generated to demonstrate that the suitability of a core that can accommodate the nearly depleted fuel assemblies in the central region of the core.

Figure 6.3 The fissile mass distribution (g of ^{235}U) of core with nearly depleted fuel assemblies on the western side of the core: Core B

Fissile mass distribution: Core with nearly depleted assemblies

		3	4	5	6	7	8	9
	Al	Be	Be	Be	Be	Be	Be	source
B	Al	Be	282.13	245.24	240.07		300.00	Mo	139.70
C	Al	Be	Mo	201.05	131.95	220.46	165.43	286.45	Hydr
D	Al	Be	192.66	172.04	133.96		239.32	Mo	138.87
E	Pb	Be	Mo	153.95	84.74	146.27	131.70	249.85	Hydr
F	Pb	Be	178.63	149.59	141.54		191.35	Mo	132.00
G	Pb	Be	Mo	238.58	88.50	162.19	166.41	286.55	Hydr
H	Pb	Be	300.00	278.86	258.73	264.50	300.00	Be	Al

BOC	Mass	7035.35
PPF		3.62
Keff		0.970356

PPF: power-peaking factor

The fissile mass distributions for 4 cores that place the nearly depleted fuel assemblies on the western side of the core are given in Appendix B. The last core as shown yielded a maximum power peaking factor of 3.62 as denoted in Figure 6.3.

6.3 Thermal fluxes

The thermal fluxes in the irradiation positions are given in Table 6.2 below for the three cores. The fluxes for the cores in column 2 and 3 of this table are still acceptable for irradiation purposes.

Table 6.2 Thermal fluxes in the irradiation positions of the 3 different cores

Location	Reference Core (Figure 6.1) $n.cm^{-2}.s^{-1}$	Core A (Figure 6.2) $n.cm^{-2}.s^{-1}$	Core B (Figure 6.3) $n.cm^{-2}.s^{-1}$
C3	**1.3×10^{14}**	**1.1×10^{14}**	**1.27×10^{14}**
E3	**1.4×10^{14}**	**1.22×10^{14}**	**1.37×10^{14}**
G3	**1.16×10^{14}**	**1.07×10^{14}**	**1.15×10^{14}**
B8	**9.77×10^{13}**	**8.9×10^{13}**	**8.18×10^{13}**
D8	**1.28×10^{14}**	**1.26×10^{14}**	**1.12×10^{14}**
F8	**1.16×10^{14}**	**1.23×10^{14}**	**1.08×10^{14}**

* FAs: Fuel assemblies

From the inspection of Table 6.2 of the thermal flux results for the cores described above, it is noticeable that flux penalties have been incurred with the change in the core configuration. Fluxes decrease between 1.56 % to 15.3 % as denoted in Table 6.3 below. Among the noteworthy explanations that can be advanced, is that in the absence of the beryllium reflectors on the western side of the core box the level of neutron leakage has increased giving rise to this change in thermal flux levels in this core. Location F8 shows an increase of 6.03 %. There is a flux tilt that can be observed from the thermal fluxes in Table 6.4. This has arisen due to the presence of fissile material on the west side of the core.

Table 6.3 Comparison between thermal fluxes in reference core with Core A.

Location	Reference Core (Figure 6.1) $n.cm^{-2}.s^{-1}$	Core A (Figure 6.2) $n.cm^{-2}.s^{-1}$	% change in thermal flux
C3	**1.3×10^{14}**	**1.1×10^{14}**	**-15.3**
E3	**1.4×10^{14}**	**1.22×10^{14}**	**-12.8**
G3	**1.16×10^{14}**	**1.07×10^{14}**	**-7.75**
B8	**9.77×10^{13}**	**8.9×10^{13}**	**-8.90**
D8	**1.28×10^{14}**	**1.26×10^{14}**	**-1.56**
F8	**1.16×10^{14}**	**1.23×10^{14}**	**+6.03**

Table 6.4 Comparison between thermal fluxes for the core box between the reference core and Core A

	Reference Core n.cm-2.s-1	Core A n.cm-2.s-1	% difference
East	1.48E+13	1.21E+13	18.24
side	2.48E+13	2.03E+13	18.15
	3.25E+13	2.65E+13	18.46
	3.78E+13	3.08E+13	18.52
	4.06E+13	3.34E+13	17.73
	3.88E+13	3.25E+13	16.24
	3.87E+13	3.33E+13	13.95
	3.43E+13	3.02E+13	11.95
	2.53E+13	2.26E+13	10.67
end	1.50E+13	1.36E+13	9.33
Poolside	2.81E+13	2.56E+13	8.90
	5.08E+13	4.69E+13	7.68
	6.59E+13	6.20E+13	5.92
	8.46E+13	8.08E+13	4.49
	9.35E+13	9.26E+13	0.96
	9.17E+13	9.35E+13	-1.96
	7.78E+13	8.12E+13	-4.37
	6.22E+13	6.78E+13	-9.00
	4.00E+13	4.57E+13	-14.25
end	2.65E+13	3.12E+13	-17.74
West	1.32E+13	2.02E+13	-53.03
side	2.64E+13	3.20E+13	-21.21
	5.42E+13	4.64E+13	14.39
	7.18E+13	7.46E+13	-3.90
	7.90E+13	7.29E+13	7.72
	7.95E+13	8.72E+13	-9.69
	7.10E+13	6.73E+13	5.21
	5.35E+13	6.38E+13	-19.25
	3.96E+13	4.73E+13	-19.44
end	2.65E+13	3.12E+13	-17.74
South	1.48E+13	1.21E+13	18.24
side	2.49E+13	2.04E+13	18.07
	3.83E+13	3.17E+13	17.23
	5.65E+13	4.72E+13	16.46
	7.11E+13	6.02E+13	15.33
	6.69E+13	5.80E+13	13.30
	5.97E+13	5.35E+13	10.39
	5.30E+13	5.02E+13	5.28
	4.58E+13	4.65E+13	-1.53
	2.47E+13	3.02E+13	-22.27
end	1.32E+13	2.02E+13	-53.03

In order to characterize the shift in flux, key peripheral positions located around the core were selected from the results file of OSCAR-3. It can also be observed that a downward

shift occurs in the thermal flux levels, which is more noticeable in the core configuration of Figure 6.2. The main contributor as mentioned above is the change in reflection of neutrons on the western side of the core.

Table 6.5 Thermal fluxes in the hydraulic rabbit position for three cores

Core	Location	Thermal flux ($n.cm^{-2}.s^{-1}$)
Reference Core	**E9**	**8.52×10^{13}**
	G9	**9.48×10^{13}**
Core A (Figure 6.2)	**C9**	**8.89×10^{13}**
	E9	**1.03×10^{14}**
	G9	**7.80×10^{13}**
Core B (Figure 6.3)	**C9**	**7.84×10^{13}**
	E9	**9.01×10^{13}**
	G9	**6.77×10^{13}**

In comparison with the reference core the thermal flux in the hydraulic rabbit position at G9 is lower by 17.7 %. On the other hand in location E9 the thermal flux level has an order of magnitude of 10^{14}, which is favourable.

Thermal fluxes at the poolside face of the reactor core are provided in Table 6.6. The trend in the thermal fluxes is similar to that in the irradiation positions of the core.

Table 6.6 Thermal flux on the poolside of the cores

Location	**Reference Core (Figure 6.1)** $n.cm^{-2}.s^{-1}$	Core A (Figure 6.2) $n.cm^{-2}.s^{-1}$	Core B (Figure 6.3) $n.cm^{-2}.s^{-1}$
H3	5.38×10^{13}	5.00×10^{13}	5.39×10^{13}
H4	6.37×10^{13}	5.96×10^{13}	6.11×10^{13}
H5	7.07×10^{13}	6.96×10^{13}	6.87×10^{13}
H6	6.90×10^{13}	7.06×10^{13}	6.52×10^{13}
H7	5.97×10^{13}	6.19×10^{13}	5.67×10^{13}

The thermal fluxes in the irradiation positions in the central irradiation positions where the rigs are placed are given in Table 6.7.

Table 6.7 Thermal flux in the rig irradiation positions

Location	**Reference Core (Figure 6.1)** $n.cm^{-2}.s^{-1}$	Core A (Figure 6.2) $n.cm^{-2}.s^{-1}$	Core B (Figure 6.3) $n.cm^{-2}.s^{-1}$
B6	1.61×10^{14}	1.46×10^{14}	1.51×10^{14}
D6	2.10×10^{14}	1.99×10^{14}	1.95×10^{14}
F6	2.00×10^{14}	2.00×10^{14}	1.89×10^{14}

Table 6.8 and Table 6.9 provide the thermal flux in the irradiation positions along in the axial direction. Fluxes are provided from layer 3 to layer 9 of the core axially. For each of the irradiation positions the peak value of the thermal flux occurs at layer six of the core. The isotope production plate should be positioned at this level in the core for optimum transmutation. The fluxes shown in these tables are those for the reference core.

The axial height of the assembly is divided into 17 layers from top to bottom with dimensions as follows:

9.0; 6.0; 5.0; 4.0; 3.0850, 4.3250; 4.3259; 4.625; 4.625; 2.7; 5.95; 5.9750; 5.9750; 4.3925; 4.3925; 6.0; 9.0 (cm)

Table 6.8 Thermal fluxes in irradiation positions, B8, D8, F8 per layer for reference core

Layer	**B8** ($n.cm^{-2}.s^{-1}$)	**D8** ($n.cm^{-2}.s^{-1}$)	**F8** ($n.cm^{-2}.s^{-1}$)
3 (19.3925 cm)	1.3×10^{14}	1.75×10^{14}	1.57×10^{14}
4 (25.3675 cm)	1.62×10^{14}	2.09×10^{14}	1.86×10^{14}
5 (31.3425 cm)	1.97×10^{14}	2.50×10^{14}	2.21×10^{14}
6 (37.2925 cm)	2.02×10^{14}	2.52×10^{14}	2.21×10^{14}
7 (39.9925 cm)	1.32×10^{14}	1.57×10^{14}	1.37×10^{14}
8 (44.6250 cm)	1.12×10^{14}	1.30×10^{14}	1.13×10^{14}
9 (49.2425 cm)	9.96×10^{13}	1.12×10^{14}	9.67×10^{13}

Table 6.9 Thermal fluxes in the irradiation positions, C3, E3, G3 per layer for reference core.

Layer	**C3** ($n.cm^{-2}.s^{-1}$)	**E3** ($n.cm^{-2}.s^{-1}$)	**G8** ($n.cm^{-2}.s^{-1}$)
3	1.86×10^{14}	1.92×10^{14}	1.56×10^{14}
4	2.28×10^{14}	2.36×10^{14}	1.91×10^{14}
5	2.80×10^{14}	2.90×10^{14}	2.35×10^{14}
6	2.94×10^{14}	3.05×10^{14}	2.47×10^{14}
7	1.96×10^{14}	2.07×10^{14}	1.66×10^{14}
8	1.75×10^{14}	1.86×10^{14}	1.83×10^{14}
9	1.64×10^{14}	1.74×10^{14}	1.40×10^{14}

Table 6.10 and Table 6.11 show the thermal fluxes in the core that is being recommended in this submission. The thermal fluxes in the recommended core although of the same order of magnitude still indicate flux penalties in comparison with the reference core. As with the reference core the maximum value of the thermal fluxes occur at layer 6 axially.

Table 6.10 Thermal fluxes in irradiation positions, B8, D8, F8 per layer for recommended core.

Layer	**B8** ($n.cm^{-2}.s^{-1}$)	**D8** ($n.cm^{-2}.s^{-1}$)	**F8** ($n.cm^{-2}.s^{-1}$)
3	1.21×10^{14}	1.74×10^{14}	1.70×10^{14}
4	1.48×10^{14}	2.08×10^{14}	2.02×10^{14}
5	1.81×10^{14}	2.50×10^{14}	2.44×10^{14}
6	1.88×10^{14}	2.59×10^{14}	2.49×10^{14}
7	1.22×10^{14}	1.64×10^{14}	1.57×10^{14}
8	1.06×10^{14}	1.38×10^{14}	1.32×10^{14}
9	9.51×10^{13}	1.21×10^{14}	1.15×10^{14}

Table 6.11 Thermal fluxes in the irradiation positions, C3, E3, G3 per layer for recommended core

Layer	**C3** ($n.cm^{-2}.s^{-1}$)	**E3** ($n.cm^{-2}.s^{-1}$)	**G8** ($n.cm^{-2}.s^{-1}$)
3	1.48×10^{14}	1.59×10^{14}	1.40×10^{14}
4	1.82×10^{14}	1.95×10^{14}	1.71×10^{14}
5	2.24×10^{14}	2.40×10^{14}	2.11×10^{14}
6	2.35×10^{14}	2.53×10^{14}	2.22×10^{14}
7	1.59×10^{14}	1.73×10^{14}	1.50×10^{14}
8	1.42×10^{14}	1.56×10^{14}	1.35×10^{14}
9	1.33×10^{14}	1.46×10^{14}	1.27×10^{14}

6.4 Fast fluxes

The intention of extracting the fast fluxes from the results file of OSCAR-3 is to provide an input value to the determination of the neutron fluence. As requested from the management of the research reactor there would be a keen interest to evaluate the effect of the proposed change in the core configuration on the reactor internals and the effect of embrittlement. With regard to this matter, it is shown in the tables below that there are significant increases in the fast flux levels. The total effect however cannot be properly treated in this investigation, as this would go beyond the scope of this dissertation. However, if there were a need to restrict the use of the core configuration for the campaign to deplete the nearly spent fuel assemblies this configuration would need to be used on a limited basis.

The increase in fast fluxes range from 5.5 % to 44.3 % (excluding fuel positions), for Core A which is more suited for the purposes of depleting the nearly spent fuel assemblies.

Table 6.12 Comparison between fast fluxes for core box between the reference core and Core A

	Reference Core n.cm-2.s-1	Core A n.cm-2.s-1	% difference
East	3.47E+12	2.83E+12	18.44
side	6.91E+12	5.61E+12	18.81
	1.08E+13	8.73E+12	19.17
	1.28E+13	1.03E+12	91.95
	1.31E+13	1.06E+12	91.91
	1.13E+13	9.32E+12	17.52
	1.09E+13	9.34E+12	14.31
	9.65E+12	8.48E+12	12.12
	6.83E+12	6.14E+12	10.10
end	3.91E+12	3.56E+12	8.95
Poolside	9.19E+12	8.43E+12	8.27
	2.67E+13	2.48E+13	7.12
	5.72E+13	5.41E+13	5.42
	7.53E+13	7.33E+13	2.66
	8.24E+13	8.21E+13	0.36
	8.17E+13	8.35E+13	-2.20
	6.80E+13	7.16E+13	-5.29
	3.66E+13	3.97E+13	-8.47
	1.81E+13	2.10E+13	-16.02
end	9.57E+12	1.15E+13	-20.17
West	3.27E+12	6.87E+12	-110.09
side	6.86E+12	1.66E+13	-141.98
	1.53E+12	3.69E+13	-2311.76
	2.39E+13	4.44E+13	-85.77
	3.01E+13	5.64E+13	-87.38
	4.14E+13	5.18E+13	-25.12
	2.70E+13	5.37E+13	-98.89
	2.10E+13	3.47E+13	-65.24
	1.77E+13	2.20E+13	-24.29
end	9.57E+12	1.15E+13	-20.17
South	3.47E+12	2.83E+12	18.44
side	6.68E+12	5.45E+12	18.41
	1.07E+13	8.85E+12	17.29
	1.78E+13	1.49E+13	16.29
	2.26E+13	1.92E+13	15.04
	1.99E+13	1.73E+13	13.07
	1.61E+13	1.44E+13	10.56
	1.50E+13	1.44E+13	4.00
	1.12E+13	1.33E+13	-18.75
	6.29E+12	1.05E+13	-66.93
end	1.32E+12	6.87E+12	-420.45

Table 6.13 Comparison between fast fluxes for different cores

Location	**Core A** ($n.cm^{-2}.s^{-1}$)	**Core B** ($n.cm^{-2}.s^{-1}$)	**% difference**
B9	6.96×10^{13}	5.21×10^{13}	+ 33.5
C9	8.40×10^{13}	6.73×10^{13}	+ 24.8
D9	1.06×10^{14}	8.07×10^{13}	Fuel
E9	9.70×10^{13}	7.47×10^{13}	+29.8
F9	1.02×10^{14}	7.53×10^{13}	Fuel
G9	6.96×10^{13}	5.63×10^{13}	+ 23.6
H9	3.89×10^{13}	3.39×10^{13}	+ 14.7

Notwithstanding the fast fluxes on the western side of the core, the fast fluxes on the opposite side show that the flux levels decrease similarly to the thermal fluxes. The increase in the fast fluxes on the western side of the core can be attributed to the closeness of fissile material to the face of the core box.

6.5 Depletion in cores

The depletion of the nearly spent fuel assemblies is depicted in Table 6.8 and Table 6.9. For Core A (Figure 6.2) the fissile mass depletes on average between 19.72 g and 20.73 g of ^{235}U during the cycle. In Core B (Figure 6.3), the average depletion is between 8.13 g and 10.88 g ^{235}U. From an operational point of view, Core A may be suitable since the fuel assemblies can be depleted with one 30-day cycle. For Core B on average the nearly spent fuel should take two 30-day cycles to deplete, depending on the initial mass.

In this regard Core A is proposed, as can also be demonstrated by the power peaking for this core is also more within the imposed constraints applied for safe operation.

Table 6.14 Depletion in central region of the core (average of 3 cycles)

Position	Mass in g	Mass in g	Mass in g	Average mass in g	Depletion rate over 30 days (g/day)
D5	19.65	20.34	21.76	20.58	0.686
E4	18.37	19.80	20.98	19.72	0.657
F5	20.32	20.48	21.39	20.73	0.691

Table 6.15 Depletion at the periphery of the core (average of 3 cycles)

Position	Mass in g	Mass in g	Mass in g	Average mass in g	Depletion rate over 30 days (g/day)
B9	8.07	8.18	8.14	8.13	0.271
D9	11.53	11.93	11.75	11.73	0.391
F9	10.94	11.08	10.63	10.88	0.362

6.6 Reactivity control parameters

In the table below it has been demonstrated that the total control rod worth for the recommended core configuration exceeds 20.0 dollar as required by the operational limits and conditions. The shutdown margin also complies with the criteria for normal operation of the research reactor.

Table 6.16 Reactivity control parameters for the reference core and the recommended core

Core	Excess reactivity (dollar)	Shut down margin (dollar)	Total control rod worth (dollar)
Reference core	10.1	22.6	32.7
Recommended core	8.2	25.2	33.4

6.7 Fuel economy

- In comparison with the reference core in this submission, Core A uses 2.40% more fuel per annum.
- In comparison with the reference core, Core B uses 2.82% more fuel per annum.

The fissile masses of fuel assemblies are subdivided into units of 20 grams in Tables 6.17 and 6.18. Heavier fuel assemblies are grouped from 261 grams to 300 grams and the lighter

fuel assemblies from 141 grams to 180 grams. The average depletion per cycle for heavier fuel assemblies is 24.56 g for the reference core. The depletion in the recommended core for heavier fuel assemblies is 21.46 g. This means that on the average heavier fuel assemblies will stay longer in the recommended core than the reference core. This, in turn, translates to a savings of HEU for this core configuration per fuel assembly.

Using Equation 3.9 to calculate the consumption rate of ^{235}U in the reactor core, the following results are obtained.

Consumption rate = $1.05(1+\alpha)$ P g/day

$\alpha = 0.169$

P = 20 MW.

Thus, consumption rate = 24.5 g/day

= 736 g/ 30-day cycle

The above value obtained represents a global calculation of the consumption rate of ^{235}U in the core. A more accurate and representative value is obtained with the OSCAR-3 depletion calculation.

Table 6.17 Breakdown by mass over the depletion range for the reference core

Range	BOC Mass (g)	EOC Mass (g)	Change in mass (g)
300-281	300.00	270.93	29.07
	300.00	278.59	21.41
280-261	278.69	258.46	20.23
	277.91	256.04	21.87
	271.63	244.01	27.62
	264.43	237.28	27.15
	Average	**300-261**	**24.56**
260-241	251.53	231.48	20.05
	250.45	229.69	20.76
	249.81	228.04	21.77
240-221	235.87	211.60	24.27
	227.60	201.24	26.36
	220.56	192.39	28.17
220-201	216.46	186.77	29.69
	209.20	184.82	24.38
	202.41	173.36	29.05
200-181	199.13	171.80	27.33
	191.67	164.07	27.60
180-161	176.87	153.16	23.71
	168.43	144.78	23.65
	167.18	142.19	24.99
160-141	153.18	132.99	20.19
	148.42	125.44	22.98
	147.76	126.55	21.21
	144.10	120.46	23.64
	Average	**180-141**	**22.91**
140-120	133.73	111.98	21.75
	132.00	109.07	22.93

Table 6.18 Breakdown by mass over the depletion range for the recommended core

Range	BOC Mass (g)	EOC Mass (g)	Mass delta
300-281	300.00	280.22	19.78
	300.00	277.19	22.81
	300.00	284.10	15.90
	285.48	264.15	21.33
280-261	278.47	257.94	20.53
	277.07	250.85	26.22
	266.22	242.58	23.64
	Average	**300-261**	**21.46**
260-241	257.01	235.61	21.40
	255.72	230.59	25.13
	255.22	233.46	21.76
	253.75	232.03	21.72
	253.27	231.47	21.80
	250.51	222.05	28.46
240-221	235.83	213.20	22.63
	228.75	203.73	25.02
220-201	218.81	189.06	29.75
200-181			
180-161	170.52	150.53	19.99
	167.14	143.51	23.63
160-141	160.66	140.69	19.97
	157.04	137.02	20.02
	154.94	132.00	22.94
	154.85	135.17	19.68
	151.47	131.26	20.21
	146.83	126.73	20.10
	142.36	123.42	18.94
	Average	**180-141**	**20.61**
140-120	131.76	113.39	18.37
	130.15	108.44	21.71
	129.90	109.58	20.32
	125.11	105.46	19.65

6.8 Summary

In the foregoing chapter, the results have been presented of the core configurations that have been investigated. These results are important from a technical point of view to establish which core configuration is suitable to answer the problem statement of Chapter 1, Section 1.2. These results serve as a platform for the Chapter 7 that advances a recommended core configuration.

CHAPTER 7 CONCLUSION AND RECOMMENDATIONS

7.1 Introduction

In this chapter, the conclusion of the investigation into the different core configurations is set out. The platform used to recommend a given core configuration is that of neutronic analysis of each core configuration. The parameters generated during the investigation will thus serve as a basis upon which the particular core will be recommended. This chapter also identifies the need for future work in this area of work.

7.2 Comparison between the two core configurations

Table 7.1 provides the parameters that are used for comparing the two cores that were investigated in this study. Firstly, the thermal flux penalties for both cores span over a similar range when compared to the reference core. The factor that makes a difference with both cores is the removal of the reflector material that gives rise to leakage at the western core box and consequently less than ideal neutron economy. The principal parameters that are taken into account in the decision-making process are the thermal flux, and the power peaking factor for the two core configurations.

An important parameter that needs to be taken into account is the power peaking factor for both cores. For the recommended fissile mass distribution with the heavier fuel assemblies on the periphery of the core, the criterion for the power peaking factor is achieved without difficulty for each reload calculation.

In the case of the depletion of the nearly spent fuel assemblies, the core of Figure 6.2 (Core A) is able to deplete a single fuel assembly (120 g to 140 g) during one operating cycle. The depletion rate of Core A was found to be 0.678 g/cycle in comparison to 0.341 g/cycle for Core B. Core B will need at least two cycles to deplete these fuel assemblies, based on the depletion rate that has been calculated. From an operational point of view, given the difficulty with the power peaking and the depletion behaviour this core operation is not sustainable.

For the core of Figure 6.3 (Core B), with the nearly spent fuel assemblies on the periphery of the core, although the power peaking can be contained careful attention and greater difficulty

is experienced to ensure that this criterion is not exceeded. The power peaking for Core B was calculated as 3.62, which exceeds the criterion of 3.5. This core therefore poses a risk that is unfavourable to the operational limits and conditions for operation of the SAFARI-1 research reactor core.

Table 7.1 Essential core parameters used in comparing different cores

Parameter	**Core A**	**Core B**
Depletion rate	0.678 g/cycle (centre of core)	0.341 g/cycle (on periphery of core)
Thermal flux penalty	1.6%-15.3%	2.2%-16.3%
Power peaking factor	3.36	3.62
Fuel economy increase	2.4 %	2.82%
Fast flux increase (western side)	5.5%-44.3%	3.71%-8.1%

The increase of the fast flux on the western side of the core box is unfavourable for the reactor internals and will give rise to an increase in the neutron fluence for the core.

7.3 Recommended core configuration

In the light of the above parameters that are provided in Table 7.1 the recommended core configuration is Core A. The basis for this core is that it complies with the operational limits and conditions for operation of SAFARI-1 reactor, having a power peaking factor of 3.36, the thermal flux penalty should borne as part of the trade off that occurs when the nearly depleted fuel assemblies, are placed in the centre of the core. The thermal flux penalty ranging between 1.6% and 15.3%, is adverse as this parameter should be kept to a minimum. The depletion rate of 0.678 g/cycle is favourable for burning these fuel assemblies for one cycle.

7.4 Future research

An effective way to improve performance of the reactor is to optimise its core layout, increasing neutron flux in the reactor channels and decreasing it fuel expenditures. Optimal locations of all fuel assemblies in the core, fuel types used, number of fuel assemblies of each type and their discharge burn-ups, as well as the number of beryllium blocks at the periphery of the core should satisfy all the safety constraints and the fuel requirements [9].

The problem stated can be characterised as a large combinatorial problem with non-linear compute-intensive objectives and constraints. Although various heuristic approaches exist to generate improved core loading patterns, they cannot provide high quality of the solutions obtained. To solve such optimisation problems and improve core management for the SAFARI-1 research reactor, research into mathematical methods appropriate to the problem should be the subject of future research [9].

Two main questions can be seen to find the best arrangement for a given set of assemblies with respect to safety and operational constraints [12]:

1.0 What is the "best arrangement" in relation to the maximum power peaking factor?

What is the optimal mathematical method that should be used to find the patterns?

There are two ways to find the best patterns. The first one consists of using expert knowledge and doing a manual search, or building expert systems. The second one requires an optimisation method that finds the best pattern without evaluating all the possible patterns [12].

Future research calls for the use of mathematical optimisation methods to be applied. Two prominent mathematical optimisation methodologies have evolved that appear to have various degrees of applicability to the nuclear fuel management decision-making problem. More classical methods such as linear, quadratic and dynamic programming have met with limited success. Stochastic methods, such as Simulated Annealing (SA) and Genetic Algorithm (GA) are well suited but carry a heavy computational burden [8]. The appropriate

mathematical optimisation method could form the subject of future research for this type of investigation.

7.5 Conclusion

The core configuration recommended is being put forward on the basis of analysis of the neutron behaviour of the core. This core is favourable in terms of the power peaking, the depletion rate, and the fuel economy in relation to the reference core. It is also crucial to take into account the technical and safety constraints under which the research reactor operates. A nuclear fuel management code is a valuable tool that assists with decision-making in this regard. It is also necessary to interpret these results with experience feedback of the reactor that has been accumulated over the years of operation. The past and current data of the reactor will give this work the necessary fidelity for appropriate implementation.

APPENDIX A

The cores selected demonstrate suitability of the core configuration with the nearly spent fuel assemblies in the central region of the core and the heavier fuel assemblies on the periphery (0403, 0404, 0405, 0406).

Core-0403

	3	4	5	6	7	8	
B	264.43	227.60	202.41		271.63		278.69
C		148.42	167.36	209.20	199.15	220.56	
D	199.13	132.00	124.50		153.18		249.81
E		133.73	108.17	147.76	164.21	167.18	
F	176.87	134.58	133.96		144.10		277.91
G		168.43	108.84	191.67	199.15	216.46	
H	300.01	251.53	235.87	250.45	300.01		

BOC Mass	7032.40
PPF	3.37
keff	0.970356

Core-0404

	3	4	5	6	7	8	9
B	277.10	231.19	199.32		286.61		300.01
C		147.28	148.29	217.91	180.37	228.51	
D	196.43	132.45	132.00		153.66		260.30
E		134.58	94.10	147.01	145.29	166.56	
F	178.53	137.28	134.88		146.27		287.41
G		173.77	96.43	190.44	180.26	227.67	
H	300.01	276.42	247.72	274.80	300.01		

BOC Mass	7112.42
PPF	3.49
keff	0.970356

Core-0405

	3	4	5	6	7	8	9
B	277.31	260.69	189.59		282.13		300.01
C		163.53	130.91	196.47	162.96	251.68	
D	184.71	132.70	132.00		170.69		275.45
E		141.96	82.19	155.26	128.32	172.04	
F	178.63	151.17	149.02		154.07		285.45
G		177.25	85.49	181.50	162.69	240.07	
H	300.01	277.15	274.80	277.13	300.01		

BOC Mass	7158.44
PPF	2.68
keff	0.970356

Core-0406

	3	4	5	6	7	8	9
B	277.07	253.74	228.75		278.47		300.01
C		154.85	147.06	235.83	199.15	253.27	
D	218.31	129.90	125.11		157.94		255.72
E		130.15	113.11	151.47	146.36	157.04	
F	167.14	142.36	131.76		146.83		285.48
G		160.66	115.49	170.52	199.15	250.51	
H	300.01	266.22	255.22	257.01	300.01		

BOC Mass	7232.62
PPF	3.36
keff	0.970356

Core-04-E6

	3	4	5	6	7	8	9
B	255.72	235.83	228.75		277.07		300.01
C		160.66	147.06	167.14	199.15	255.78	
D	157.04	151.47	125.11		218.81		257.01
E		131.76	113.11	130.15	146.36	250.51	
F	154.94	142.36	129.90		154.94		285.48
G		170.52	115.49	146.83	199.15	266.22	
H	300.01	278.47	253.27	253.75	300.01		

BOC Mass	7232.62
PPF	3.36
keff	0.969180

Core-04-E7

	3	4	5	6	7	8	9
B	242.58	231.47	230.59		277.19		300.01
C		189.06	130.71	203.73	180.44	250.85	
D	178.63	146.24	124.73		222.07		257.94
E		138.87	99.11	133.96	128.99	232.08	
F	153.95	141.96	132.00		162.19		284.12
G		213.20	102.86	143.29	180.44	264.15	
H	300.01	280.22	233.46	235.61	300.01		

BOC Mass	7199.90
PPF	3.17
keff	0.970356

Core-04-E8

	3	4	5	6	7	8	9
B	241.77	215.64	213.05		278.31		300.01
C		192.10	115.35	204.39	162.48	250.49	
D	189.79	162.19	132.00		208.11		259.91
E		141.96	86.81	138.87	113.70	220.85	
F	165.56	143.29	133.96		175.99		284.17
G		205.59	91.78	156.62	163.70	263.82	
H	300.01	280.00	226.08	237.07	300.01		

BOC Mass	7128.46
PPF	3.03
keff	0.970356

The following cores have been provided to demonstrate minimal changes in the fissile mass distribution and should reach optimum performance over a short period of time (04-E6, 04-E7, 04-E8).

APPENDIX B

The cores selected demonstrate that the core configuration with nearly spent fuel assemblies on the periphery of the core is feasible (0D01, 0D02, 0D03).
However the loading arrangement in regard to the fissile mass distribution requires careful analysis in order to prevent unacceptable power peaking.

Core-0D01

			3	4	5	6	7	8	9
	Al	Be	Be	Be	Be	Be	Be	Be	source
B	Al	Be	264.43	227.60	220.56		300.00	Mo	134.58
C	Al	Be	Mo	199.13	167.36	202.41	199.15	271.63	Hydr
D	Al	Be	191.67	167.18	124.50		216.46	Mo	132.00
E	Pb	Be	Mo	148.42	108.17	144.10	164.21	235.87	Hydr
F	Pb	Be	168.43	147.76	133.73		176.87	Mo	133.96
G	Pb	Be	Mo	209.20	108.84	153.18	199.15	277.91	Hydr
H	Pb	Be	300.00	251.53	249.81	250.45	278.69	Be	Al

BOC Mass	7032.45
PPF	3.49
keff	0.970356

Core-0D02

			3	4	5	6	7	8	9
	Al	Be	Be	Be	Be	Be	Be	Be	source
B	Al	Be	264.43	227.60	220.56		278.69	Mo	134.58
C	Al	Be	Mo	199.13	167.36	202.41	199.15	271.63	Hydr
D	Al	Be	191.67	167.18	124.50		216.46	Mo	132.00
E	Pb	Be	Mo	148.42	108.17	144.10	164.21	235.87	Hydr
F	Pb	Be	168.43	147.76	133.73		176.87	Mo	133.96
G	Pb	Be	Mo	209.20	108.84	153.18	199.15	277.91	Hydr
H	Pb	Be	300.00	251.53	249.81	250.45	300.00	Be	Al

BOC Mass	7032.45
PPF	3.45
keff	0.970356

Core-0D03

			3	4	5	6	7	8	9
	Al	Be	Be	Be	Be	Be	Be	Be	source
B	Al	Be	274.80	238.71	228.14		300.00	Mo	139.70
C	Al	Be	Mo	188.59	148.73	194.10	182.24	286.45	Hydr
D	Al	Be	185.21	165.25	132.00		220.82	Mo	138.87
E	Pb	Be	Mo	155.14	95.43	146.27	147.19	245.24	Hydr
F	Pb	Be	173.17	151.17	141.96		175.18	Mo	134.58
G	Pb	Be	Mo	202.70	98.01	156.62	181.71	286.55	Hydr
H	Pb	Be	300.00	260.30	253.90	259.87	300.00	Be	Al

BOC Mass	7062.06
PPF	3.19
keff	0.970356

Fissile mass distribution: Core with nearly depleted assemblies

			3	4	5	6	7	8	9
	Al	Be	Be	Be	Be	Be	Be	Be	source
B	Al	Be	282.13	245.24	240.07		300.00	Mo	139.70
C	Al	Be	Mo	201.05	131.95	220.46	165.43	286.45	Hydr
D	Al	Be	192.66	172.04	133.96		239.32	Mo	138.87
E	Pb	Be	Mo	153.95	84.74	146.27	131.70	249.85	Hydr
F	Pb	Be	178.63	149.59	141.54		191.35	Mo	132.00
G	Pb	Be	Mo	238.58	88.50	162.19	166.41	286.55	Hydr
H	Pb	Be	300.00	278.86	258.73	264.50	300.00	Be	Al

BOC	Mass	7035.35
PPF		3.62
Keff		0.970356

REFERENCES

[1] J.J. Duderstadt, L.J. Hamilton, "Nuclear Reactor Analysis", John Wiley & Sons, 1976.

[2] H.W. Graves, "Nuclear Fuel Management", John Wiley & Sons, 1979.

[3] Safety of Research Reactors, No. NS-R-4, IAEA, 2005.

[4] D.I. Tomasevic, "Modern Nodal Diffusion Methods in Nuclear Reactor Analysis and Design", Proceedings of YUNSC Conference, Belgrade, Yugoslavia, 1,77, 1996.

[5] G.Ball, "Efficient use of Neutrons at SAFARI-1," Trans.Intl.Conf.Research Reactor Fuel Management (RRFM'99), Bruges, Belgium, 29-31 March 1999.

[6] F. Reitsma, E.Z. Muller, "Evaluation of the Use of Nodal Methods for MTR Neutronic Analysis," Proceedings of the 17th International Meeting on Reduced Enrichment for Research and Test Reactors, Williamsburg, Virginia, USA, 18-23, 1994.

[7] E.Z. Muller, G. Ball, W.R. Joubert, H.C. Schutte, C.C. Stoker, F. Reitsma, "Development of a Core Follow Calculational System for Research Reactors," Proceedings of the 9th Pacific Basin Nuclear Conference, Sydney, Australia, 1-6 May 1994.

[8] P.J. Turinsky, P.M. Keller, H.S. Abdel-Khalik, "Evolution of Nuclear Fuel Management and Reactor Operational Aid Tools," Nuclear Engineering and Technology, Volume 37, No.1, February 2005.

[9] Y.P. Mahlers, "Core Management and Calculational Tools for the WWR-M Research Reactor in Ukraine," Proceedings of an International Conference on Research Reactor, Utilization, Safety, Decommissioning, Fuel and Waste Management, Santiago, Chile, 10-14 November 2003.

[10] A. Lerner, M. Madariaga, R. Waldman, "Conceptual Analysis of the Fuel Management Strategy for the RA-3 Research Reactor at 10 MW," Proceedings of the 2004 International RERTR Meeting, Vienna, Austria, 7-12 November 2004.

[11] G. Ball, "Calculational Support Provided to SAFARI-1", AFRA Regional Conference on Research Reactor Operation, Utilisation and Safety, Algiers, 10-11 April 1999.

[12] J. Arguad, "A loading Pattern Optimization Method for Nuclear Fuel Management," Report number EDF-DER-97-NB-00004, 1992-1998.

[13] A.J. D'Arcy, SAFARI-1 Safety Analysis Report, Document No. RR-SAR-0017, May 2002.

[14] F. Reitsma, W.R. Joubert, "A Calculational System to Aid Economical Use of MTRs, International Conference on Research Reactor Fuel Management (RRFM' 99), Bruges, Belgium, 29-31 March 1999.

[15] Neutron Irradiation Embrittlement of Reactor Pressure Vessel Steels, Technical Report Series No. 163, 1975.

[16] K. Farrell, "Assessment of Aluminium Structural Materials for Service within the ANS Reflector Vessel," ORNL/TM-130049, August 1995.

[17] J.R. Lamarsh, "Introduction to Nuclear Engineering", Addison-Wesley Publishing Company, Second Edition, 1983.

[18] N. Guessous, F. Hadfat, "Analytical Nodal Methods for Diffusion Equations," Electronic Journal of Differential Equations, Conference 11, pp. 143-155, 15 October 2004.

[19] South African Nuclear Energy Corporation, "OSCAR-3, User's Manual", 2002.

[20] R.D. Lawrence, "Progress in Nodal Methods for the Solution of the Neutron Diffusion and Transport Equations", Prog. In Nuclear Energy, Volume 17, pp. 271-301, 1986.

[21] L.E. Moloko et al, "Improvement and Validation of OSCAR-3 Usage in SAFARI-1 Core Modelling," 2006.